Cryptoclidus eurymerus humerus and femur finite element structure analyses inform on plesiosaur muscle forces and flipper twisting (#58478)

First submission

Guidance from your Editor

Please submit by 7 Apr 2021 for the benefit of the authors (and your \$200 publishing discount).



Structure and Criteria

Please read the 'Structure and Criteria' page for general guidance.



Author notes

Have you read the author notes on the guidance page?



Raw data check

Review the raw data.



Image check

Check that figures and images have not been inappropriately manipulated.

Privacy reminder: If uploading an annotated PDF, remove identifiable information to remain anonymous.

Files

Download and review all files from the <u>materials page</u>.

7 Figure file(s)

5 Table file(s)

2 Raw data file(s)

Structure and Criteria



Structure your review

The review form is divided into 5 sections. Please consider these when composing your review:

- 1. BASIC REPORTING
- 2. EXPERIMENTAL DESIGN
- 3. VALIDITY OF THE FINDINGS
- 4. General comments
- 5. Confidential notes to the editor
- Prou can also annotate this PDF and upload it as part of your review

When ready <u>submit online</u>.

Editorial Criteria

Use these criteria points to structure your review. The full detailed editorial criteria is on your guidance page.

BASIC REPORTING

- Clear, unambiguous, professional English language used throughout.
- Intro & background to show context.
 Literature well referenced & relevant.
- Structure conforms to <u>PeerJ standards</u>, discipline norm, or improved for clarity.
- Figures are relevant, high quality, well labelled & described.
- Raw data supplied (see <u>PeerJ policy</u>).

EXPERIMENTAL DESIGN

- Original primary research within Scope of the journal.
- Research question well defined, relevant & meaningful. It is stated how the research fills an identified knowledge gap.
- Rigorous investigation performed to a high technical & ethical standard.
- Methods described with sufficient detail & information to replicate.

VALIDITY OF THE FINDINGS

- Impact and novelty not assessed.
 Negative/inconclusive results accepted.
 Meaningful replication encouraged where rationale & benefit to literature is clearly stated.
- All underlying data have been provided; they are robust, statistically sound, & controlled.
- Speculation is welcome, but should be identified as such.
- Conclusions are well stated, linked to original research question & limited to supporting results.

Standout reviewing tips



The best reviewers use these techniques

	n
	N

Support criticisms with evidence from the text or from other sources

Give specific suggestions on how to improve the manuscript

Comment on language and grammar issues

Organize by importance of the issues, and number your points

Please provide constructive criticism, and avoid personal opinions

Comment on strengths (as well as weaknesses) of the manuscript

Example

Smith et al (J of Methodology, 2005, V3, pp 123) have shown that the analysis you use in Lines 241-250 is not the most appropriate for this situation. Please explain why you used this method.

Your introduction needs more detail. I suggest that you improve the description at lines 57-86 to provide more justification for your study (specifically, you should expand upon the knowledge gap being filled).

The English language should be improved to ensure that an international audience can clearly understand your text. Some examples where the language could be improved include lines 23, 77, 121, 128 – the current phrasing makes comprehension difficult. I suggest you have a colleague who is proficient in English and familiar with the subject matter review your manuscript, or contact a professional editing service.

- 1. Your most important issue
- 2. The next most important item
- 3. ...
- 4. The least important points

I thank you for providing the raw data, however your supplemental files need more descriptive metadata identifiers to be useful to future readers. Although your results are compelling, the data analysis should be improved in the following ways: AA, BB, CC

I commend the authors for their extensive data set, compiled over many years of detailed fieldwork. In addition, the manuscript is clearly written in professional, unambiguous language. If there is a weakness, it is in the statistical analysis (as I have noted above) which should be improved upon before Acceptance.



Cryptoclidus eurymerus humerus and femur finite element structure analyses inform on plesiosaur muscle forces and flipper twisting

Anna Krahl Corresp., 1, 2, 3, Andreas Lipphaus 1, Paul Martin Sander 3, Ulrich Witzel 1

Corresponding Author: Anna Krahl

Email address: annakrahl1@googlemail.com

Background. Plesiosauria (Sauropterygia) are secondarily marine Diapsida. They are the only tetrapods that evolved hydrofoil fore- and hindflippers. Once this locomotory specialization had evolved, it remained essentially unchanged for 135 Ma. It is still contentious whether plesiosaurs flew underwater, rowed, or employed a mixture of both styles. Long bones of Tetrapoda experience torsion, bending, and compression during locomotion. Load case superposition indicates that bones are loaded primarily by compression. Thus, it is possible to use finite element analyses as a test environment for hypotheses of muscle lines of action (LOA), if the objective is to receive a homogenous compressive stress distribution and to optimize for bending minimization. **Methods.** To study locomotion in plesiosaurs, a Cryptoclidus eurymerus (Middle Jurassic Oxford Clay of the UK) humerus and femur were analyzed with FE methods according to this concept. Based on muscle reconstructions that had been undertaken earlier, LOA were deduced experimentally for all humerus and femur muscles of *Cryptoclidus*. These were acquired by spanning threads into a cast of a fore- and hindflipper of a mounted skeleton. LOA and muscle attachments were conveyed to a meshed volumetric model of the humerus and femur that were created from micro-CT scans. By computing the compressive stress distribution for two load cases, down- and upstroke, for each bone, muscle forces were approximated by stochastic iteration. **Results.** After the reconstruction of a flipper twisting mechanism driven by muscles and the addition of those extensors and flexors in the finite element models that originate from humerus and femur and contribute to flipper twisting, a homogenous compressive stress distribution was obtained. Humeral and femoral elevators and depressors, powering underwater flight and not rowing, were found to have the highest muscle forces. Extensors and flexors exert high muscle forces in

Biomechanics Research Group, Chair of Product Development, Faculty of Mechanical Engineering, Universitätsstr. 150, Ruhr-Universität Bochum, 44801 Bochum, Germany

² Fachbereich Geowissenschaften, Hölderlinstraße 12, Eberhard-Karls-Universität Tübingen, 72074 Tübingen, Germany

Institute of Geoscience, Section Paleontology, Nußallee 8, Rheinische Friedrich-Wilhelms Universität Bonn, 53115 Bonn, Germany



comparison to Cheloniidae. This corroborates a myological flipper twisting mechanism in plesiosaurs complementing hydrodynamic studies that showed that flipper twisting is crucial for plesiosaur underwater flight.



1 Cryptoclidus eurymerus humerus and femur finite

2 element structure analyses inform on plesiosaur

muscle forces and flipper twisting

4 5 6

3

Anna Krahl¹², Andreas Lipphaus¹, Paul Martin Sander³, Ulrich Witzel¹

7

- 8 ¹ Biomechanics Research Group, Chair of Product Development, Faculty of Mechanical
- 9 Engineering, Ruhr-University Bochum, Universitätsstr. 150, 44801 Bochum, Germany
- 10 ² Fachbereich Geowissenschaften an der Eberhard-Karls-Universität Tübingen, Hölderlinstraße
- 11 12, D-72074 Tübingen
- 12 ³ Institute of Geoscience, Section of Paleontology, Rheinische Friedrich-Wilhelms Universität
- 13 Bonn, Nußallee 8, 53115 Bonn, Germany

14

- 15 Corresponding Author:
- 16 Anna Krahl¹
- 17 Email address: anna.krahl@uni-tuebingen.de

18 19

Abstract

- 20 Background. Plesiosauria (Sauropterygia) are secondarily marine Diapsida. They are the only
- 21 tetrapods that evolved hydrofoil fore- and hindflippers. Once this locomotory specialization had
- evolved, it remained essentially unchanged for 135 Ma. It is still contentious whether plesiosaurs
- 23 flew underwater, rowed, or employed a mixture of both styles. Long bones of Tetrapoda
- 24 experience torsion, bending, and compression during locomotion. Load case superposition
- 25 indicates that bones are loaded primarily by compression. Thus, it is possible to use finite
- 26 element analyses as a test environment for hypotheses of muscle lines of action (LOA), if the
- 27 objective is to receive a homogenous compressive stress distribution and to optimize for bending
- 28 minimization.
- 29 Methods. To study locomotion in plesiosaurs, a Cryptoclidus eurymerus (Middle Jurassic
- 30 Oxford Clay of the UK) humerus and femur were analyzed with FE method coording to this
- 31 concept. Based on muscle reconstructions that had been undertaken earlier, LOA were deduced
- 32 experimentally for all humerus and femur muscles of Cryptoclidus. These were acquired by
- 33 spanning threads into st of a fore- and hindflipper of a mounted skeleton. LOA and muscle
- 34 attachments were conveyed to a meshed volumetric model of the humerus and femur that were
- 35 created from micro-CT scans. By computing the compressive stress distribution for two load
- 36 cases, down- and upstroke, for each bone, muscle forces were approximated by stochastic
- 37 iteration.
- 38 **Results.** After the reconstruction of a flipper twisting mechanism driven by muscles and the
- 39 addition of those extensors and flexors in the finite element models that originate from humerus



and femur and contribute to flipper twisting, a homogenous compressive stress distribution was obtained. Humeral and femoral elevators and depressors, powering underwater flight and not rowing, were found to have the highest muscle forces. Extensors and flexors exert high muscle forces in comparison to Cheloniidae. This corroborates a myological flipper twisting mechanism in plesiosaurs complementing hydrodynamic studies that showed that flipper twisting is crucial for plesiosaur underwater flight.

46 47

48 49

50

51

52

53

54

55

56 57

58 59

60 61

62

63

64

65

66

67 68

69

70

71

72

73

74 75

76

77

78 79

Introduction

Plesiosaur musculoskeletal apparatus and locomotion

Cryptoclidus eurymerus osteology



Plesiosauria are secondarily aquatic Tetrapoda that roamed the marine realm from the Late Triassic (Wintrich et al., 2017) until the K/Pg mass extinction (Bardet, 1994; Motani, 2009; Vincent et al., 2011; Vincent et al., 2013; Bardet et al., 2014). Plesiosauria form the most derived group of Sauroptervgia. The origin of Sauroptervgia remains obscure. They could have evolved from basal archosauromorphs (Merck, 1997) or lepidosauromorphs (Rieppel & Reisz, 1999), or they may be the sister taxon to archosauromorphs and lepidosauromorphs (Neenan, Klein & Schever, 2013). The most striking and unique key innovation of plesiosaurs is that they have evolved four similarly-looking wing-like flippers by the Late Triassic (Wintrich et al., 2017). All four flippers are dorsoventrally flattened, have greatly foreshortened zeugopodium (< one-third of autopodium length), and form a hydrofoil (Robinson, 1975, 1977). They possibly had an asymmetrical profile (Robinson, 1975; Caldwell, 1997) like the flippers of recent underwaterflying Spheniscidae and Chelonioidea. Unlike plesiosaurs, Spheniscidae, Chelonioidea, Cetacea, and Otariinae have only evolved hydrofoil-like foreflippers (Walker, 1973; Schreiweis, 1982; Feldkamp, 1987; Fish & Battle, 1995; Fish, 2004; Cooper et al., 2007; Elliott et al., 2013). Sea turtle, penguin, and sea lion hindflippers evolved into paddles (Shufeldt, 1901; Walker, 1971b; Davenport, Munks & Oxford, 1984) and are employed in steering and terrestrial and aquatic locomotion (Walker, 1971b; Pinshow, Fedak & Schmidt-Nielsen, 1977; Clark & Bemis, 1979; Davenport, Munks & Oxford, 1984; Feldkamp, 1987; Wyneken, 1997). Whale hindlimbs are almost entirely reduced. Scapula, coracoid, pubis, and ischium of plesiosaurs lie ventrally and meet the element from the other side in the body midline in a slightly v-shaped configuration. Coracoid and pubis are much expanded. The dorsal expansion of the scapula and the dorsally directed ilium are much reduced (Andrews, 1910). Gastralia lie in between the pectoral and the pelvic girdle and stiffen the trunk region (Sues, 1987; Taylor, 1989). Humeri and femora of Cryptoclidus eurymerus have a nd proximal end, an oval midshaft cross section, and the epicondyles are expanded and hammer-shaped (Andrews, 1910; personal observation on IPB R324, a Cryptoclidus eurymerus exhibit (Oxford Clay, Middle Jurassic, UK) at the Goldfuß Museum, Rheinische Friedrich-Wilhelms-Universität Bonn).

The dis expansion of the humerus of *Cryptoclidus* is larger than that of the femur and rather untypical for most plesiosaurs (compare to e.g., Großmann, 2006, Sachs, Hornung & Kear, 2016). Radius/ulna, and tibia/fibula are much shortened and rather disc-like in appearance





(Andrews, 1910). Metacarpal V and metatarsal V have been moved proximally into the rows of carpals and tarsals (Robinson, 1975). Fore- and hindflippers are hyperphalangic (Andrews, 1910).

83 84

80

81

82

85

86

87

88

89

90

91 92

93

94

95

96

97

98

99

100

101102

103

104

105106

107

108

109110

111

112

113

114

Plesiosaur muscle reconstructions

Plesiosaur muscles have been reconstructed by Watson (1924), Tarlo (1958), Robinson (1975), Lingham-Soliar (2000), Carpenter et al. (2010), Araújo & Correia (2015), and by Krahl (2020). Carpenter et al. (2010) Araújo & Correia (2015), and Krahl (2020) relied on the extant phylogenetic bracket (EPB), a method that emerged in the 1990s which provides reliable inferences for soft tissue anatomy of fossils (Bryant & Russel, 1992; Wittmer, 1995). Older studies (Watson, 1924; Tarlo, 1958; Robinson, 1975; Lingham-Soliar, 2000) did not employ the EPB and did not clearly state which extant taxa they relied on for their muscle reconstructions. Muscles that originate on the pectoral girdle and insert into the humerus or span it have been reconstructed by Watson (1924), Tarlo (1958), Robinson (1975), Lingham-Soliar (2000), Carpenter et al. (2010), Araújo & Correia (20 🗐 and by Krahl (2020). Locomotor muscles which arise from the pelvic girdle, traverse the femur, and attach to the femur have been partially reconstructed by Robinson (1975), Lingham-Soliar (2000), and Carpenter et al. (2010) and completely by Krahl (2020). Muscles which arise distally from the humerus and femur have been partially reconstructed by Robinson (1975) and entirely by Krahl (2020). Robinson (1975) seems to have reconstructed the ventral side of the foreflipper and the dorsal side of the hindflipp although thus is not clearly stated (Robinson, 1975; Krahl, 2020). The possible implication is that the dorsal and ventral fore- and hindflipper sides could look the same in plesiosaurs is unsubstantiated by the B as dorsal and ventral fore- and hindlimb musculature of extant Sauropsida is not symmetrical (Walker, 1973; Meers, 2003; Russell & Bauer, 2008; Suzuki et al., 2011). The distal plesiosaur fore- and hindflipper musculature reconstructed by Robinson (1975) looks very similar to the cetacean foreflipper musculature in terms of how extremely reduced it is (Cooper et al., 2007). This whale-like state appears unlikely for plesiosaurs, as cetacean foreflippers are merely control surfaces and not hydro for s (Fish, 2002; Woodward, Winn & Fish, 2006) while the main propulsive organ of whales is a large muscular swimming tail with a fluke (Fish, 1996; Woodward, Winn & Fish, 2006). Contrastingly, plesiosaurs actively swam with their fore- and hindflippers (Krahl, 2020). Krahl (2020) are the first who reconstructed the entire locomotor musculature of a plesiosaur fore- and hindflipper. They reconstructed a complex array of muscles for fore- and hindflipper of plesiosaurs which enables the plesiosaur to twist both its flipper pairs along the flipper length and maybe even actively control the flipper profile, as hydrodynamic computations of plesiosaurs by Witzel, Krahl & Sander (2015) and Witzel (2020) suggest.

115116117

118

119

Plesiosaur locomotion

The locomotory style of plesiosaurs has been an ongoing debate since over one century (Williston, 1914; Watson, 1924; Tarlo, 1958; Robinson, 1975, 1977; Feldkamp, 1987; Lingham-



Soliar, 2000; Carpenter et al., 2010; Araújo et al., 2015; Araújo & Correia, 2015; Liu et al., 2015; Krahl, 2020). It has been suggested that plesiosaurs row like ducks or otters (Williston, 1914; Watson, 1924; Tarlo, 1958; Araújo et al., 2015; Araújo & Correia, 2015), fly underwater like sea turtles and penguins (Robinson, 1975, 1977; Lingham-Soliar, 2000; Carpenter et al., 2010; Liu et al., 2015; Krahl, 2020), or use rowing-flight like sea lions (Feldkamp, 1987; Liu et al., 2015). The main difference between the different locomotory styles results from the underlying hydrodynamics: In rowing, water drag is used to push the body forward while in underwater flight, lift produced by the onflowing water travelling around a cambered flipper profile is used (e.g., Baudinette & Gill, 1985; Fish, 1996; Walker & Westneat, 2000). The rowing-flight of sea lions relies on both hydrodynamic mechanisms, drag-based and lift-based, at different phases of the limb cycle (Fellik mp, 1987). It was also proposed that the foreflipper pairs employ a different mode of locomotion (Tarlo, 1958; Lingham-Soliar, 2000; Liu et al., 2015).

A flipper used in rowing is mostly moved in anteroposterior direction with little dorsoventral motion (Pace, Blob & Westneat, 2001; Rivera, Rivera & Blob, 2011; Rivera, Rivera & Blob, 2013). The anteroposterior expansion and the dorsoventral reduction of the bony elements of the plesiosaur pectoral and pelvic girdle, as well as the accompanying reduction or hypertrophy of locomotory muscles have been interpreted as being in favor for protraction and retraction of the flipper, i.e., a rowing motion (Watson, 1924; Tarlo, 1958; Godfrey, 1984).

Contrastingly, during underwater flight, the flipper is beaten mainly in dorsoventral direction with a minor anteroposterior component. The flipper downstroke of Chelonioidea and Spheniscidae is characterized by major depression and minor retraction of the flipper. The upstroke is performed by humeral elevation and protraction. The flipper tip describes a skew "O" in anterodorsal-posteroventral direction (Clark & Bemis, 1979; Davenport, Munks & Oxford, 1984; Rivera, Wyneken & Blob, 2011; Rivera, Rivera & Blob, 2013). As Robinson (1975) noted, the hydrofoil-shaped flippers of plesiosaurs, tapering towards the tip_z superficially comparable to that of penguins and sea turtles, imply that they were used for underwater flight and not for rowing. Also, the glenoid and acetabular shape of plesiosaurs restrict movement in anteroposterior direction more than in dorsoventral direction (Krahl, 2020).

During rowing flight, the downstroke is lift-generating and similar to the downstroke of the underwater fliers. At the point of maximum flipper depression, the flipper is turned around like a paddle and pushes against the water during its retraction and elevation. During the recovery stroke, the flipper is brought back anteriorly and dorsally, possibly also producing propulsion by lift (Feldkamp, 1987). Godfrey (1984) found that in recent underwater fliers, the shoulder girdles are characterized by a strong bony support expanding in the dorsoventral direction, which is not present in plesiosaurs. Therefore, he noted that there is more similarity between sea lions and plesiosaurs than with recent "true" underwater fliers (Godfrey, 1984).

Besides the locomotory style, it is still being discussed how the four flippers were moved in relation to each other, i.e., fore- and hindflipper synchronously, asynchronously, or out of phase. This debate is based on the so called four-wing problem which addresses how plesiosaurs



avoided placing their hindflippers into the vortices shed by their foreflippers which would mean a considerable performance decrease of the hindflippers (Frey & Riess, 1982; Tarsitano & Riess, 1982; Lingham-Soliar, 2000; Carpenter et al., 2010; Muscutt et al., 2017).

162163164

165166

167

168

169170

171172

173174

175

176

177

178

179180

181 182

183 184

185

186 187

188

189

190

191 192

193

194

160

161

Muscle physiology

During a limb motion cycle, muscles may follow either a shortening-stretch cycle or a stretch-shortening cycle. During the former, the muscle is shortened while its force output increases. Then, the muscle is stretched and the force output decreases. During the latter, the muscle is stretched at the beginning while its force output increases. When the muscle contracts, its force output drops (Rassier, MacIntosh & Herzog, 1999). Muscle force production depends on muscle architecture. Muscle architecture includes muscle length and tendon (if present) length, lines of action, muscle mass, specific density of muscle, intrinsic muscle strength, fascicle length, and pennation angles (Alexander & Vernon, 1975; Gans, 1982; Sacks & Roy, 1982; Powell et al., 1984; Narici, Landoni & Minetti, 1992; Anapol & Barry, 1996; Kummer, 2005; Azizi, Brainerd & Roberts, 2008). Parallel-fibred muscles have on average longer fascicles, a larger volume, and can contract faster (which depends on the fibre type composition) than pennate muscles. However, more muscle fibres can be arranged adjacently to each other in a pennate muscle than in a parallel-fibred muscle of the same size. Thus, a pennate muscle can exert a higher force than a same-sized parallel-fibred muscle, although the pennate muscle has shorter fibres. This is so because the exerted maximum muscle force does not only depend on the fibre length but also on the physiological cross sectional area (PCSA), i.e., the sum of fibre cross sections (Gans, 1982; Burkholder et al., 1994; Allen et al., 2010; Hug, Wall & Taylor, 2015).

Also, muscle length of a parallel-fibred, fast contracting muscle (or one close to it) varies substantially and is traded off for a high metabolic intake and a relatively low force production. Contrastingly, strongly pennated muscles exert relatively high forces at markedly lower metabolic costs but are much slower contracting and have poor fibre contraction control (Biewener & Roberts, 2000).

Pennate muscles may develop relatively high forces while their muscle lengths behave almost isometrically (e.g., turkey (musculus (m.) gastrocnemius) (Roberts et al., 1997) or wallaby (m. gastrocnemius, m. plantaris) (Biewener, Konieczynski & Baudinette, 1998). Contrastingly, the fan-shaped m. pectoralis, which has a very high initial power output, shows a very great muscle length change of 30-40% for *Columba liva* (Biewener, Corning & Tobalske, 1998; Biewener & Roberts, 2000) or approximately 30% for *Anas platyrhynchos* (Williamson, Dial & Biewener, 2001). Generally, muscle length change of vertebrate striated muscle may span up to +/- 25% (contraction and stretching in relation to resting length (=0%)) before its capability to generate force drops markedly (Biewener & Roberts, 2000).

195196197

198

199

Finite element structure analysis

As strain gauge measurements demonstrate, long bones of Tetrapoda are functionally loaded fluctuatingly by torsion, compression, and bending (Biewener & Dial, 1995; Carrano,





209

210

211212

213

214

215

216

217

218

219220

221

222

223224

225

226

227

228

229230

231

232233

234

235236

237

238

239

200 1998: Blob & Biewener, 1999: Lieberman, Polk & Demes, 2004: Main & Biewener, 2004, 2007: Butcher et al., 2008; Butcher & Blob, 2008; Sheffield et al., 2011; Young & Blob, 2015; Young 201 et al., 2017). They are mostly loaded by bending in alternating directions or primarily by 202 compression and subordinately by tension (Biewener & Dial, 1995; Blob & Biewener, 1999; 203 204 Lieberman, Polk & Demes, 2004; Main & Biewener, 2004; Butcher et al., 2008; Butcher & Blob, 2008; Sheffield et al., 2011). High torsional loads are imposed on terrestrial tetrapod long 205 bones (Biewener & Dial, 1995; Carrano, 1998; Blob & Biewener, 1999; Main & Biewener, 206 2004, 2007; Butcher et al., 2008; Butcher & Blob, 2008; Sheffield et al., 2011). 207

To reflect such changing loading conditions, a number of loadcases can be analyzed with finite element structure analysis (FESA; Witzel & Preuschoft, 2005) and then be superimposed on each other (Carter, Orr & Fyhrie, 1989). By reducing the bending moment (Klenner et al., 2015; Lutz et al., 2016; Milne, 2016; McCabe et al., 2017; Lipphaus & Witzel, 2018), biological lightweight structures may evolve (Klenner et al., 2015). FESA is used in different disciplines encompassing engineering sciences and biomechanics (Rayfield, 2007). FESA allows analysis of mechanical stresses and strains in technical and biological structures in 2-D or 3-D (Rayfield, 2007; Witzel et al., 2011) and may add to our understanding of the function of bony elements (Witzel et al., 2011). Compressive loads are applied to the bone via tension chords. Tension chords are either muscles (active tension chord) or ligaments (passive tension chords), and they act in pairs of agonists and antagonists (Witzel & Preuschoft, 2005; Sverdlova & Witzel, 2010; Curtis et al., 2011; Witzel et al., 2011; Klenner et al., 2015; Felsenthal & Zelzer, 2017). A movement is powered by the agonist while the antagonist opposes it to fulfill a controlled movement (Sverdlova & Witzel, 2010). If the same movement is inverted, the agonist becomes the antagonist and vice versa. Thus, agonists and antagonists load a bony structure constantly by compressive stress, although the agonist is exerting proportionally a higher force than the antagonist.

The aim of this study was to test plesiosaur muscle reconstructions with FESA. So, the muscle reconstructions obtained with the EPB, i.e., based on comparative anatomical studies, were cross-checked with the mechanically imposed demands on muscles. We evaluated how muscle physiological details, such as muscle length changes can contribute to muscle reconstructions of fossils and whether FESA of the plesiosaur humerus and femur can inform on plesiosaur locomotion. The results complement earlier hydrodynamic studies that implied that plesiosaurs must have used flipper twisting for efficient underwater flight (Witzel, Krahl & Sander, 2015; Witzel, 2020) and corroborate the myological flipper twisting mechanism reconstructed by Krahl (2020).

Materials & Methods

Analog model of lines of action

Lines of action (LOA) represent the direct connection in a straight line between a muscle's origin and insertion (Krahl et al., 2019). They were experimentally attained in an analog model (Figure 1) with the help of casts of the pectoral (Figure 2, 3) and pelvic girdle and



251

252253

254

255

256257

258

259

260

261262

263

264

265266

267

268

269270

271

272

273

274

275

276

277

278279

240 limbs (Figure 4, 5) of the Cryptoclidus eurymerus specimen (IGPB R 324) on exhibition in the Goldfuß Museum, Division of Paleontology, Institute of Geosciences, Rheinische Friedrich-241 Wilhelms-Universität Bonn. The casts of the pectoral and pelvic girdle were mounted on a 242 wooden frame and fixed with screws. In place of the vertebral column, which also serves as 243 244 origin of locomotory muscles, wooden bars were screwed. The anatomical positioning of the casts and the vertebral colum e based on the mounting of IGPB R 324. Thick styrofoam was 245 used to replace the missing cartilage capping in the shoulder and hip joint. The fore- and 246 hindflipper were hung into the construction and the respective joint with the help of the muscle 247 lines of action. Supportively, the flippers were fixed by additional ropes in the chosen flipper 248 249 positions (Figure 1).

To physically model the lines of action, non-elastic thread was used. Screw eve pins were screwed into the cast at the muscle origin and insertion surfaces. Muscle attachments of all locomotory muscles of the fore- and hindflipper that span either glenoid or acetabulum (12 on foreflipper, 14 on hindflipper) were adopted from Krahl (2020). Each thread was strung through three electrical terminal strips. Next, hooks were tied to both ends of the threads, which were then hooked into the screw eyes representing muscle origins and insertions (Figure 1). If a muscle attachment surface is small, the screw eye pin was screwed approximately in the middle of it. Contrastingly, muscles with large attachment areas were subdivided into several subportions to better encompass the varying fiber insertion angles and directions and to obtain more evenly distributed compressive stresses in the FE models. Correspondingly, the total muscle force of a muscle was subdivided, too, and fractions of the total muscle force were assigned to the subportions. Usually, the most anterior and posterior points in the body midline were chosen for placement of the screw eye pins (e.g., m. subcoracoscapularis, m. coracobrachialis brevis, m. pectoralis). In the case of, e.g., m. latissimus dorsi, a position in between the cranialmost and caudalmost origin was chosen. This is done in order to represent those portions that are supported the best by EPB (cranial and middle portion) but also to cover the less well supported portion (caudal) (Krahl, 2020).

These subportions do not necessarily represent actual partitions of the reconstructed muscles, although some muscles may have likely been compartementalized, e.g., m. pectoralis, m. latissimus dorsi, m. puboischiofemoralis internus, and m. puboischiofemoralis externus. Muscles with two or more heads (i.e., m. deltoideus scapularis, m. deltoideus clavicularis, m. coracobrachialis brevis, m. coracobrachialis longus, m. triceps brachii, m. caudifemoralis brevis (ilium and vertebral column), m. flexor tibialis internus, m. flexor tibialis externus, m. puboischiofemoralis internus, and m. puboischiofemoralis externus were assigned two (or more) threads. The resultant vector of the various subportions of those muscles that have a large origin area went into the FE models. Agonistically and antagonistically acting muscles that insert into, originate from, or span the humerus (Table 2) and femur (Table 3) were devised from the mount. Pictures were taken for documentation from cranial/anterior (Figure 2 a-f; Figure 4 a-f), caudal/posterior (Figure 3 a-f; Figure 5 a-f), ventral (Figure 2 g, h; Figure 4 g, h) and dorsal (Figure 3 g, h; Fig 5 g, h). In Figure 2 g) and h), Figure 3 g) and h), Figure 4 b), g), and h), and



Figure 5 g), h) some muscles are pictured that do not run relatively close to either humerus, femur, or the flipper. This is due to measuring muscle length changes in the analog model. The FESA are based on sketches in which we presumed force vectors for the respective muscles that were on average lying closer to the adjacent bony elements. These muscles were possibly held close by annular pulleys. Limb cycle movement terminology follows Rivera, Wyneken & Blob (2011) and Krahl (2020) who used humeral and femoral depression, elevation, protraction, and retraction, which reflect the requirements for underwater flight well.

OI.

Changes in muscle length

Three positions in the fore- and hindflipper beat cycle were chosen to measure the total muscle length change for muscles that originate on the pectoral and pelvic girdle or the vertebrae and insert into or span the humerus and femur. These positions are the maximum dorsal excursion of the fore-/hindflipper during the upstroke (~+50° to the horizontal) (Figure 2 a, b; Figure 3 a, b; Figure 4 a, b; Figure 5 a, b), maximum ventral excursion of the fore-/hindflipper during the downstroke (~-50°) (Figure 2 e, f; Figure 3 e, f; Figure 4 e, f; Figure 5 e, f), and the neutral position (0°) (Figure 2 c, d; Figure 3 c, d; Figure 4 c, d; Figure 5 c, d). Based on the orientation of glenoid and acetabulum, the tip of the foreflipper points slightly forward, the hindflipper tip points slightly backward. Protraction and retraction were not considered because, based on the osteology, they contribute minorly to the flipper beat cycle. Also, in this study we examined basically whether or not total muscle length changes may add value for muscle reconstructions of extinct vertebrates.

Flipper range of motion has been determined before by Carpenter et al. (2010) and Liu et al. (2015) for various plesiosaur species, but the results depend greatly on how much cartilage is presumed to have been capping the humerus and femur and the glenoid and acetabulum, as indicated by Liu et al. (2015), and on the species (which differ in size of the dorsal tuberosity/trochanter). The authors presumed that the humeral and femoral head of *Cryptoclidus* (IGPB R 324) were capped by thick vascularized cartilage comparable to that described for *Dermochelys coriacea* (Rhodin, Ogden & Conlogue, 1981; Snover & Rhodin, 2008). This is based on the observation that the proximal bone surfaces of both, the humerus and femur of *Cryptoclidus* (IGPB R 324), are pierced by large vascular canals and are very similar looking to the proximal humeral head of *Dermochelys* (Rhodin, Ogden & Conlogue, 1981; Snover & Rhodin, 2008; Krahl, 2020.

The authors refrained from calling the neutral flipper position the resting position of the flipper because it is probably impossible to determine the flipper resting position for an extinct species. Furthermore, in the muscle physiological literature, the term resting length" usually refers to individual sarcomeres (Rassier, MacIntosh & Herzog, 1999) or fascicles of a muscle (Biewener & Roberts, 2000). Moreover, not-to know the exact flipper resting length influences the exact value of muscle stretching and contraction but not the end result of total length change of a muscle which was calculated in this study (s_r below). This is because the absolute values of



muscle stretching and contraction are measured in relation to the neutral position but the total muscle length change is the difference between maximum muscle stretching and contraction.

All three positions of the fore- and hindflipper were successively fixed with ropes suspended from the wooden frame holding the casts. For each of the three states, the optimal length of each muscle was fixed with the help of the terminal strips. Afterwards, each muscle was removed and all three muscle lengths, i.e., maximum excursion during downstroke, neutral position, and maximum excursion during downstroke were measured with a measuring tape in cm. Length changes between maximum excursion at downstroke and the neutral position as well as between maximum excursion at upstroke and the neutral position were expressed first in cm and then in %, by setting resting length as 100%. Next, muscle stretching, muscle contraction, and the difference between both, the total length change of muscle, were calculated in % (Table 1). Bar graphs for total muscle length changes in % were plotted with Microsoft Excel (Figure 6 b). Some muscle length changes were recorded as 0 cm because the actual changes in length could not be measured because they were smaller than the width of the terminal strips. In one case, i.e., m. deltoideus scapularis, it was found that the total muscle length change with an insertion on the lateral scapula blade was unphysiologic (see below), another origin area (from the ventrolateral scapula) was tested and shown to give physiologically plausible results that were then measured for all three positions.

FESA and muscle force determination by computation

The right humerus and left femur of IGPB R 324 were scanned with the micro-CT scanner at the author's institution with an industrial high-resolution computed tomography (μ CT) scanner (model phoenix v|tome|x s 240, produced by General Electric Phoenix X-ray, Wunstorf, Germany). The scans were processed with the dedicated software datos|x and the program VGStudio MAX (Volume Graphics) to obtain image stacks in the z direction.

The image stack was loaded into Simpleware ScanIP 5.1 (Krahl et al., 2019) for further processing. For each image, the bone tissue was selected and segmented out with the help of grey scale intervals and a model was generated (Data S1 and Data S2). Next, the model was imported into ANSYS 16.0 (ANSYS Inc., Canonsberg, PA, USA). The measured dimensions of the humerus and femur of IGPB R 324 were used to scale the respective volumetric model. Next, proximal articular cartilage, respectively the glenoid/acetabular articulation surface, were modelled. The FE models were created with the element type SOLID92. The humerus model consists of 92665 elements and the femur model of 75784 elements. In the humerus, the cartilaginous articular structure is formed by 19927 elements and by 15472 elements in the femur. Bearings were placed on all nodes of the proximal surface of the cartilage models for a different research project which will not be addressed further in the current study. In both FE models, bone was modelled with a Young's modulus of 5 MF

LOA, and attachment angles were figured in sketches of humerus (Figure 7 a) and femur (Fig. 7 e) in anterior, posterior, dorsal, and ventral view that were implemented in the FE models





as vectors (Figure 7 b, f). Two- or more headed muscle bellies were tered in the FE model in form of the resultant vector. Two-joint muscles add to the counterforce. Radius and ulna/tibia and fibula exert the counterforce on the epicondyles of the humerus and femur. Two-joint muscles of the foreflipper are the m. triceps brachii and the m. biceps brachii. Two-joint muscles of the hindflipper are the m. ambiens, m. pubotibialis, m. flexor tibialis externus, m. flexor tibialis internus, m. iliotibialis, m. iliofibularis, and m. puboischiotibialis. As it is impossible to perform curved vectors in ANSYS 16.0., muscle wrappings were modelled by dividing their lines of action into several smaller straight vectors.

The force transmission on the distal articular surfaces of humerus and femur due to muscular activity was first applied in one point. This resulted in very high localized stress peaks. Therefore, force transmission was split up into several application points scattered over the distal articulation surfaces to receive a more realistic simulation of the load transmission via a surface.

Forces of each humerus and femur muscle were approximated stochastically. The distribution of compressive stress was computed for both long bones (Figure 7, c, d, g, h). Then, another run was prepared by maximizing compressive stresses and minimizing bending moments. These steps were repeated until a homogenous compressive stress distribution was obtained. This way, muscle forces were iteratively approximated (Table 3 and Table 4) (Witzel & Preuschoft, 2005; Sverdlova & Witzel, 2010).

Load case generation

Two load cases, downstroke and upstroke, were chosen to be computed to reflect the constantly varying loading regime of humerus and femur during the flipper beat cycle. For both load cases, a position was chosen in which the humerus is held horizontally at the level of the glenoid pointing laterally and slightly anteriorly, as indicated by the analog model. Similarly, the femur was positioned horizontally at the level of the acetabulum. Its flipper tip points mostly laterally but is also slightly angulated posteriorly. During the downstroke, the humerus and femur were rotated anteriorly downward along their long axis by approximately 19° (Witzel, Krahl & Sander, 2015; Witzel, 2020). During the upstroke, the humerus and femur were rotated back and about 19° posteriorly downward around their long axis (Witzel, Krahl & Sander, 2015; Witzel, 2020).

For the implementation of load cases, it is crucial to identify and consider which muscles act as agonists and antagonists (Witzel & Preuschoft, 2005). The shoulder and hip joint possibly allowed a minor clearance for rotation and protraction/retraction and a major clearance for elevation and depression stabilized by the interplay of agonists and antagonists. Muscle functions for identification of agonists and antagonists (Table 2 and Table 3) are taken from Krahl (2020). The downstroke load case is powered mainly by the humeral and femoral depressors, but also by retractors and those muscles enabling a slight downward rotation of the flipper leading edges. Flexors arising from the humerus and femur are active during the downstroke, flexing the digits and contributing to the twisting of the foreflipper and hindflipper along the flipper lengths. The upstroke load case is powered largely by humeral and femoral elevators. Humeral and femoral



protraction and rotation of the flipper leading edge upward add to the upstroke as well. The extensors which originate from the distal humerus and femur aid in flipper twisting and extension of the digits during the upstroke (Krahl, 2020).

Results

Mechanically controlled plesiosaur muscle reconstructions

Humerus musculature

Humerus muscles that were reconstructed on a biological basis (Krahl and Witzel, 2020) are counterchecked for their functionality on a mechanical basis. Musculus deltoideus scapularis was reconstructed on the anteroventral scapula posterior to m. deltoideus clavicularis and anteriorly to m. supracoracoideus and on the lateral median scapular blade. Here we can confidently reject an origin from the blade, as a total muscle length change of 70% suggests extreme muscle shortening that it is physiologically impossible (see below) (Figure 6 a; Table 1).

Myological reconstruction suggests an m. biceps brachii origin on the posterior ventral coracoid. Musculus biceps brachii and m. brachialis could either insert via a shared tendon into the proximal radius or into the posteroproximal radius and the anteroproximal ulna. Further, m. triceps brachii originates anteriorly to anterodorsally from the bony ridge surrounding the glenoid on the scapula and from the coracoid just posterior to the glenoid and inserts (well substantiated by the EPB) into the posterodorsal ulna. The posterodors at almar insertion of m. triceps brachii is unquestionable based on the EPB, and the posterior origin of m. biceps brachii is quite well supported as well. In contrast, origin areas of m. triceps brachii are debatable as well assumptions: our FESA was much improved when the m. biceps brachii/m. brachialis insertion was placed on the proximal and ventral radius and when the m. triceps brachii origin anterior to anterodorsally to the glenoid facet was more pronounced by a higher muscle force. An origin of the m. triceps brachii from the coracoid provides only a little to no lever arm and was therefore possibly reduced or lost.

Myological reconstruction suggests the insertions of m. coracobrachialis brevis and m. coracobrachialis longus due to the presence of osteological correlates on the posterior to posteroventral humeral shaft as observed in lepidosaurs (Russell & Bauer, 2008). This decision is not well supported by the EPB which would rather suggest an insertion ventrally into the intertrochanteric fossa as seen in turtles and crocodilians (Walker, 1973; Meers, 2003; Suzuki & Hayashi, 2010). A shift of their humeral insertions further distally along the shaft, is mechanically favorable as it increases the lever arms and took place comparably in Cheloniidae (Walker, 1973; Krahl et al., 2019).

Musculus scapulohumeralis anterior was not reconstructed based on myology because this muscle is only present in lepidosaurs and therefore weakly supported by EPB. However, we formulate a description and a reconstruction of this muscle below, because it adds a needed proximal rotatory component to the humeral locomotory musculature. Musculus scapulohumeralis anterior has no synonyms and is only reported for Lepidosauria (Russell &



441

450

451

454

456 457

458

459

460 461

462

463

464 465

466

467

468 469

470

471

472

473

474

475

476

477 478

Bauer, 2008). Musculus scapulohumeralis anterior has two portions which originate from the anterior ventrolateral scapula and from the posterolateral scapula, dorsal to the glenoid (in 440 Varanus exanthematicus, Iguana iguana; Jenkins & Goslow, 1983; Russell & Bauer, 2008). For plesiosaurs, it is reconstructed to originate on the anterior edge of the lateral scapula, on the base 442 443 of the scapular blade and on the posterior edge of the scapular blade. The lines of action support the latter origin because the former would result in a wrapping of m. scapulohumeralis anterior 444 around the lateral scapular blade and around the musculature that suspends the pectoral girdle 445 from the trunk, which seems rather unlikely. Yet, the origin on the posterior scapular blade 446 would also only be able to support a very small muscle belly because the scapular blade-is very 447 much reduced in comparison to archosaurs, lepidosaurs, and turtles in general (Walker, 1973; 448 Meers, 2003; Russell & Bauer, 2008; Suzuki & Havashi, 2010). This means m. scapulohumeralis 449 anterior is expected to contribute with a relatively low muscle force to propulsion. Musculus scapulohumeralis anterior inserts proximally and posterodorsally into the lepidosaur humerus, 452 relatively proximally to the latissimus dorsi (Jenkins & Goslow, 1983; Russell & Bauer, 2008). Thus, a possible m. scapulohumeralis anterior insertion could be found proximally and 453 posterodorsally, rather proximal to the m. latissimus dorsi insertion on the dorsal tuberosity of the C. eurymerus humerus associated with the strong rugosities on the dorsal humeral tuberosity. 455

Femur musculature

Femur musc e- econstructions followed biological principles and are counterchecked in the following chapter for their functionality. An m. ambiens origin site on the pubic tubercle is well supported by the EPB. An origin ventrally below the acetabulum would also be well substantiated by the EPB. From a mechanical point of view, the former has a much better lever arm than the latter, due to the rearrangement of pubis and ischium into almost ventrally flat lying plates. Therefore the m. ambiens origin site below the acetabulum can be rejected.

The m. iliofemoralis origin was reconstructed on the lateral ilium. Krahl (2020) also discuss a weakly supported option by EPB (only supported by turtles) that m. iliofemoralis origin area may have spread onto the vertebral column (Zug, 1971; Walker, 1973). An origin on the vertebral column would improve the lever arm of this muscle. Further, when the femur is depressed, m. iliofemoralis parallels and wraps around the dorsal trochanter of the femur and therefore exerts compressive stress onto it. The ilium is much reduced in size, comparable to the scapula blade. This would either indicate a much reduced ife or support its origin site shift onto the vertebral column which in turn would not limit its size in such a way.

Four origin areas are equally possible for m. puboischiofemoralis internus according to EPB: a large origin area on most of the dorsal pubis, a smaller origin on the anterodorsal ischium, a small origin area on the medial and ventral ilium, and an origin on the vertebral column. LOA of m. puboischiofemoralis internus show that they wrap around the dorsal trochanter of the plesiosaur femur. This means that m. puboischiofemoralis internus contributes substantially to femoral elevation. A large pubic portion and the ischiadic and vertebral column portion paralleling the dorsal trochanter can be substantiated from a mechanical standpoint. An



iliac origin seems to be rather unlikely because it would wrap around the femoral trochanter and than around the anterior ilium. Then due to the reduction of the ilium, this portion can only be small. Further, total muscle shortening length shows this muscle has a bad performance. All of this indicates that an iliac origin of m. puboischiofemora is internus is at least mechanically unlikely. The reconstructed iliac origin has a rather bad lever arm and shows no muscle shortening while the one from the vertebral column with a greater lever arm would be certainly favorable from a mechanical point of view.

M. gastrocnemius internus originating from the tibial epicondyle is equally well supported as an origin on the distal tibial epicondyle and the proximal tibia by EPB. FESA shows clearly that an origin similar to that of m. gastrocnemius externus, rather proximally on the tibial epicondyle at the point where the femur flairs anterodistally and posterodistally should be favored because otherwise it would be problematic to load the expanded femoral epicondyle by compressive stress in the FESA (see below).

Agonists and antagonists

Humerus musculature

Musculus coracobrachialis brevis, m. coracobrachialis longus, m. biceps brachii, the large posterior portions of m. pectoralis, m. subcoracoscapularis, m. supracoracoideus, and m. latissimus dorsi are humeral retractors. They oppose the humeral protractors which are m. deltoideus clavicularis, m. deltoideus scapularis, and the small anterior portions of m. supracoracoideus, m. subcoracoscapularis, and m. latissimus dorsi. Musculus deltoideus scapularis, m. subcoracoscapularis, m. latissimus dorsi and possibly to a very minor degree m. triceps brachii, m. scapulohumeralis anterior, and m. scapulohumeralis posterior power elevation of the humerus. The humeral depressors m. supracoracoideus, m. coracobrachialis brevis, m. coracobrachialis longus, m. deltoideus clavicularis, m. biceps brachii, and m. pectoralis act antagonistic to them. M. triceps brachii, the smaller anterior portion of m. subcoracoscapularis, the large posterior portion of m. pectoralis, m. biceps brachii, m. scapulohumeralis anterior, m. scapulohumeralis posterior, and m. deltoideus clavicularis contribute to downward rotation of the foreflipper leading edge. Functionally antagonistic are m. deltoideus scapularis, m. coracobrachialis brevis, m. corabcobrachialis longus, the larger posterior portion of m. subcoracoscapularis, and m. latissimus dorsi (Table 2).

Further sub-groupings of agonistic and antagonistic muscles are possible: The small anterior portion of m. latissimus dorsi (weak elevation and protraction) opposes the large posterior m. pectoralis portion (strong retraction and depression) in function. The small anteriorly lying m. pectoralis portion (protractor and depressor) and the large posterior m. latissimus dorsi portion (strong elevator and retractor) act as agonist and antagonist. Musculus subcoracoscapularis and m. deltoideus scapularis which elevate and protract the humerus find their functional antagonists in m. coracobrachialis brevis, m. coracobrachialis longus, m. biceps brachii, and the posterior portion of the m. supracoracoideus which depress and retract it. The large posterior portion of m. subcoracoscapularis acts as humeral elevator and retractor and the



520

521

522523

524

525

526

527528

529 530 531

532

533

534

535

536

537

538

539

540 541

542

543

544 545

546

547

548 549

550

551

552

553

554

555

556

557 558 anterior portion of m. supracoracoideus and m. deltoideus clavicularis operate oppositional to them as humeral depressors and protractors (Table 2).

Muscles that originate from the humerus aid in flipper twisting (Krahl, 2020): Musculus flexor carpi ulnaris may offset the ulnar side of carpus relatively to the humerus ventrally (or flex metacarpal V) while m. extensor carpi ulnaris and humeral m. triceps brachii could both offset the ulna in the opposite direction and the former could possibly extend metacarpal V. Musculus flexor carpi radialis can either flex metacarpal I or offset the radial side of the plesiosaur carpus ventrally. Musculus brachialis, and m. pronator teres also contribute to the latter function. These are antagonistically matched by antagonistic m. supinator longus + m. extensor carpi radialis. M. flexor digitorum longus (flexion of digit I to V) is opposed by m. extensor digitorum communis and the digital extensors (extension of digits) (Table 2).

Femur musculature

Elevators of the hindflipper are m. puboischiofemoralis internus, m. iliotibialis, m. iliofemoralis, m. iliofibularis, m. caudifemoralis brevis, m. caudifemoralis longus, m. flexor tibialis externus (portion from ilium), m. flexor tibialis internus (portion from vertebral column). Musculus puboischiofemoralis externus, m. adductor femoris, m. ischiotrochantericus, m. puboischiotibialis, m. flexor tibialis externus (portion from ischium), and m. flexor tibialis internus (ischial portion) act as femoral depressors. Protractors are m. puboischiofemoralis externus (pubic portion), m. puboischiofemoralis internus (portion from pubis and from vertebral column), m. ambiens, and m. pubotibialis. Retractors of the hindflipper are m. puboischiofemoralis externus (ischial portion), m. puboischiofemoralis internus (ischial and iliac portion), m. adductor femoris, m. ischiotrochantericus, m. iliofemoralis, m. iliotibialis, m. iliofemoralis, m. caudifemoralis brevis, m. caudifemoralis longus, m. flexor tibialis externus, and m. flexor tibialis internus. Downward rotation of the flipper leading edge during the downstroke is enabled by the agonists, m. puboischiofemoralis internus (pubis portion), m. puboischiofemoralis externus (ischium portion), m. caudifemoralis brevis, m. caudifemoralis longus, m. ambiens (if femur elevated), m. ischiotrochantericus, m. iliofibularis (as long as fibula below origin), m. puboischiotibialis, m. pubotibialis (if femur elevated), m. flexor tibialis internus, and m. flexor tibialis externus. The agonists are opposed by the antagonistically acting m. iliotibialis, m. ambiens (if femur depressed), m. pubotibialis (if femur depressed), m. iliofemoralis, m. puboischiofemoralis internus (ischial and iliac portion small), and m. puboischiofemoralis externus (pubis portion large) (Table 3).

Further, the muscles can be assigned to the following subgroups: The m. puboischiofemoralis internus originating from the dorsal pubis and vertebral column is opposed by muscles originating from the ventral ischium (m. puboischiofemoralis externus (ischial portion), m. adductor femoris, and the ischial portions of m. flexor tibialis internus and m. flexor tibialis externus). The pubic portion of m. puboischiofemoralis externus, m. ambiens, and m. pubotibialis that arise from the ventral pubis have muscles from the ilium and posterior vertebral column as antagonists (m. flexor tibialis internus and m. flexor tibialis externus, m. iliofibularis,



m. iliotibialis, m. iliofemoralis, m. puboischiofemoralis internus (ischial portion)). Musculus ambiens and m. pubotibialis have m. iliofibularis as antagonist. Musculus femorotibialis and m. extensor digitorum longus arise mostly dorsally from the femur. Musculus gastrocnemius externus, m. gastrocnemius internus, and m. flexor digitorum longus arise ventrally from the femur. Musculus gastrocnemius externus and m. gastrocnemius internus, and flexor digitorum longus (flexion of digits) seem to oppose m. extensor digitorum longus (extension of digits) and m. femorotibialis (Table 3).

Muscle physiology and FESA

Muscle forces and FESA

Humerus

The compressive stress distribution and the muscle forces were computed for loadcase downstroke and upstroke of the humerus FE model. In initial FESA runs, the dorsal tuberosity of the humerus was left unloaded. Augmenting the FESA with the muscle wrapping of m. latissimus dorsi and m. subcoracoscapularis around the dorsal tuberosity revealed by LOA observations aided in loading this process with compressive stress. In addition, extensors and flexors that wrap around the anterior and posterior distal curved expansions (ectepicondylar and entepicondylar processes) of the humerus allowed to load them by compressive stress. Muscles that wrap around bone impose compressive stress onto it. Contrastingly, muscles that do not wrap around bone impose solely localized tensile loads onto the bone.

In the FESA results for the human rus (Figure 7 c, d), red, orange, and yellow correspond with low compressive stress (0 to -3.6 MPa). The dorsal tuberosity of the humans, as well as large parts of its distal expansions, are loaded by low compressive stress. This corresponds well with the observation that the distal humans is mostly composed of spongy bone that is covered only by a thin layer of cortical bone (compare to Krahl, 2020). The green colour spectrum correlates with moderate compressive stress (-3,6 to -7,2 MPa). Large areas of the cortical and spongy bone, especially in the region of the humans shaft, but also in smaller regions of the distal expansions are compressed moderately (Figure 7 c, d). Turquoise to blue colours conform to high compressive stress (-7,2 to -10,8 MPa). High compressive stress partially corresponds to the outermost cortical layer. Especially the proximal region of the head and the proximal shaft are loaded by high compressive stress (Figure 7 c, d).

On the distal articulation surface of the humerus, high stress peaks occur very narrowly localized (Figure 7 c). These are artifacts which are due to the application of the counterforce. The counterforce was applied scattered over the large distal articulation surface, instead of applying it to one point, to receive a more realistic force induction. Nevertheless, this is a trade off between realistic conditions and technical software possibilities.

During the downstroke, m. pectoralis is the muscle that develops the highest muscle force (9600 N) among the muscles that span the glenoid. Surprisingly, during the upstroke, m. pectoralis still develops a higher force (5267 N) than either one of the main humerus elevators, i.e., m. latissimus dorsi and m. subcoracoscapularis. Nonetheless, both develop high muscle



 forces, m. subcoracoscapularis (4422 N) and m. latissimus dorsi (3918 N), to sustain the upstroke together. Generally, it becomes apparent, that greater muscle forces are produced by retractors and depressors of the humerus than by its elevators and protractors. Furthermore, extensors and flexors develop partially extremely high muscle forces, with m. flexor carpi radialis producing 8460 N during the downstroke and m. extensor digitorum communis producing 6000 N during the upstroke (Table 4).

Femur

For loadcase downstroke and upstroke of the femur FE model, the compressive stress distribution and the muscle forces were computed. In initial FESA runs of the femur, we were unable to load the dorsal trochanter and the distal epiphyses of the femur with compressive stress because the muscles would simply pull away from their origin. Thereby only localized tensile loads were observable in FESAs. Then we again introduced the LOA observations on muscle wrapping, with m. iliofemoralis and m. puboischiofemoralis internus wrapping around the dorsal trochanter and the extensor and flexors wrapping around the distally much expanded femoral epicondyles, and the respective structures were loaded by compressive stress.

The colour coding of the compressive stress distribution in the plesiosaur femur (Figure 7 c, d) is the same as for the humerus (see above). Low compressive stress correlates mostly with the medullary region in the mid to distal femur and the distal expansions of the femur. Moderate compressive stress occurs mostly in regions where cortical bone is found, especially on the outer femur shaft. The high compressive stress values correspond mostly with areas of the femoral head and part of the cortical bone of the proximal shaft (Figure 7 g, h). Like in the FESA of the humerus, localized compressive stress peaks on the distal articulation surface of the plesiosaur femur derive from the selective application of the counterforce in several points scattered across the articulation surface (see above) (Figure 7 g).

The muscle forces of the many two-joint muscles (m. pubotibialis, m. puboischiotibialis, m. flexor tibialis externus, m. flexor tibialis internus, m. ambiens, m. iliotibialis, m. iliofibularis) in the plesiosaur hindflipper cannot be determined because they influence the femur only indirectly by adding to the counterforce. During the downstroke, m. puboischiofemoralis externus produces the highest muscle force (7878 N). During the upstroke, m. puboischiofemoralis internus produces up to 7611 N. Extensor and flexor muscle forces are considerably lower in the femur than in the foreflipper. M. gastrocnemius, a flexor, develops a total force of up to 1176 N (Table 5).

Changes in muscle length

Muscles that are dorsal to the glenoid and acetabulum extend during the downstroke and contract during the upstroke. Muscles that originate ventrally to glenoid and acetabulum contract when the humerus and femur are depressed during the downstroke and are extended during the upstroke when the humerus and femur are elevated.

Total muscle length changes of the foreflipper vary between 0% and $\overline{70}$ 87%. Three muscle (or portions thereof) (m. deltoideus clavicularis, m. triceps brachii (anterior and posterior



 portion) show no length change, i.e., the length changes were immeasurable with the technique employed here, meaning they are smaller than 1,7 cm (breadth of the terminal strips). Musculus coracobrachialis brevis (posterior portion) shows very little muscle shortening (3,88%). Otherwise, total muscle length changes cover the whole physiological spectrum, from around 9% in the posterior portion of m. subcoracoscapularis to 37% for the anterior portion of m. latissimus dorsi. The only muscle that stands out is ds with a total length change of over 70%. This is clearly not physiological. So a screw eye pin was alternatively screwed into the origin area of the m. deltoideus scapularis that is on the ventral to ventrolateral scapula anterior to the glenoid. The total muscle length change was measured again in all three flipper positions and ranged now within the measuring error, i.e., it ranged well within physiological boundaries (Table 1).

Total muscle length change for the hindflipper ranges from 0% to 35,8%. Musculus caudifemoralis brevis (ilium portion) and m. pubotibialis lack any length change due to methodical reasons (see above). Further, m. caudifemoralis brevis which originates from the vertebral column shows little total muscle length change at 5,2% while the muscle with the largest change (35,82%) in total muscle length is the portion of the m. puboischiofemoralis internus originating at the vertebral column (Table 1).

Looking at agonistic and antagonistic muscles, the total length changes of m. pectoralis and m. latissimus dorsi, the two muscles that mainly power down- and upstroke of the foreflipper, are fairly similar: the anterior portion of m. latissimus dorsi (36,96%) and m. pectoralis posterior portion (35,65%) and posterior m. latissimus dorsi portion (21,92%) and m. pectoralis anterior portion (18,75%). Total muscle length changes of agonists and antagonists were expected to be similar due to their opposing functions. Instead it was found that those muscles that show comparable total muscle length changes are rather determined by their geometric arrangement in relation to the glenoid or acetabulum. This means; that a muscle that originates from e.g. the posteroventral ischium (e.g. m. puboischiofemoralis externus (23,55%)) shows a rather similar shortening as one that originates from the anterodorsal pubis (m. puboischiofemoralis internus (21,04%)).

Discussion

Myology

As noted earlier, the muscle reconstructions on which this study is based on were obtained by evaluating comparative anatomical data (i.e., with the EPB) (Krahl, 2020). These biologically derived muscle reconstructions are counterchecked on whether they also meet the mechanical criteria to which muscles are subjected. Mostly we find that the reconstructed muscles are in accordance with the mechanical criteria, too. Although some changes of the plesiosaur fore- and hindflipper muscle reconstructions were-made due to mechanical reasons (m. biceps brachii, m. deltoideus scapularis, m. gastroenemius internus), i.e., in terms of receiving a more homogenous compressive stress distribution in FESA of the humerus and femur. We found mechanical evidence of support for some reconstructions made by Krahl (2020) which were rather weakly supported by the EPB (i.e., m. subcoracoscapularis from the



681

682

683 684

685

686

687

688

689

690

691

692 693

694

695

696

697

698

699 700

701 702

703 704

705 706

707

708

709 710

711

coracoid, m. coracobrachialis brevis, m. coracobrachialis longus, m. ambiens, m. iliofemoralis, m. puboischiofemoralis).

One muscle, m. scapulohumeralis anterior was reconstructed additionally to Krahl (2020), as it could aid in humerus rotation. Convergently to Cheloniidae (Krahl et al., 2019), muscles were found that wrap around the humerus as well as the femur in plesiosaurs. The area of origin of m. scapulohumeralis anterior is situated on the anterior scapular blade. In comparison to the reconstruction by Araújo & Correia (2015), it is not as much ventral and more laterally situated. Robinson (1975) and Watson (1924) reconstructed its attachment surface on the medial and ventral scapula which is not supported by the EPB (Jenkins & Goslow, 1983; Russell & Bauer, 2008). Contrastingly, Carpenter et al. (2010) reconstructed a large origin area of m. scapulohumeralis anterior on the lateral scapula. Instead, we reconstructed a large m. deltoideus scapularis in roughly the same area which is better substantiated by the EPB (Walker, 1973; Meers, 2003; Russell & Bauer, 2008; Suzuki & Hayashi, 2010). The results presented here disagree with Tarlo (1958) in that the origin of m. scapulohumeralis anterior is on the anteroventral scapula because this is not supported by extant Sauropsida (Walker, 1973; Meers, 2003; Russell & Bauer, 2008; Suzuki & Hayashi, 2010). The sketches of the muscle reconstructions by Lingham-Soliar (2000) are solely schematic. It is impossible to determine exact muscle attachments from these drawings. Yet, judging by the geometrical arrangement, his muscle reconstructions resemble our results. M. scapulohumeralis anterior occurs exclusively in lepidosaurs and neither in turtles nor in crocodilians (Walker, 1973; Meers, 2003; Russell & Bauer, 2008; Suzuki & Hayashi, 2010). It inserts posterodorsally into the humerus in lepidosaurs; therefore, according to the EPB this pattern was transferred to the plesiosaur in this study. None of the previous authors who have reconstructed this muscle, reconstructed its insertion in this place. They either placed it at the anterodorsal humerus (Watson, 1924; Tarlo, 1958; Robinson, 1975) or at the dorsal humerus (Lingham-Soliar, 2000; Carpenter et al., 2010).

M. scapulohumeralis anterior is reconstructed in agreement with Tarlo (1958) and Watson (1924) to potentially protract the humerus subordinately and to rotate it (Watson, 1924; Tarlo, 1958). Watson (1924) and Tarlo (1958) disagree on how protraction and rotation took place. Whereas Watson (1924) proposed the muscle to rotate the humerus anteriorly upwards, Tarlo (1958) infers the opposite. Whereas Tarlo (1958) and Robinson (1975), and the current study agree on the direction of humerus rotation, Robinson (1975) additionally describes sha as a depressor, which contradicts the results of this study. A possible minor elevational function was not described by any previous author.

712713714

715

716

717 718

719

Muscle physiology

Total muscle length changes

Total muscle length changes were calculated for glenoid and acetabulum spanning muscles and tested whether they lie within physiological boundaries. The total muscle length change of m. deltoideus scapularis, if it would have originated from the lateral scapula, is not physiological and would not allow the muscle to produce much power (compare Biewener &



Roberts, 2000) (Table 1: Figure 6 a). This could indicate, that the muscle reconstruction of m. deltoideus scapularis on the scapula blade by Krahl (2020) is wrong, despite being well supported by the EPB, and that its origin could have been restricted to the ventral side of scapula. An origin of m. deltoideus scapularis on the ventral to ventrolateral scapula anterior to the glenoid would result in a length change that is within the physiological limits (Table 1). Further, a muscle length change within the measuring error, i.e., a small one, would actually account better for the often non-parallel and rather complex architecture of the deltoid muscle (s. e.g., Krahl et al., 2019; Walker, 1973; Meers, 2003; Russell & Bauer, 2008). A reduction of the m. deltoideus scapularis from the scapular blade would mean that no locomotory muscles attach to the lateral scapular blade in plesiosaurs anymore. Solely muscle attachments that suspend the shoulder girdle remain on the scapular blades esides aquatic adaptation (Krahl et al., 2019), this could be another explanation for why the dorsal scapular projection is so much smaller than in extant Sauropsida (compare to Walker, 1973; Meers, 2003; Russell & Bauer, 2008; Suzuki & Hayashi, 2010) and potential functional analogues (compare to Walker, 1973; English, 1977; Schreiweis, 1982; Louw, 1992; Cooper et al., 2007). Similarly, a relocation or reduction of muscles originating from the ilium (e.g., m. iliofemoralis), could free or mostly free the ilium of locomotory musculature and therefore allow its reduction.

For several muscles (e.g., m. deltoideus clavicularis, the two m. triceps brachii, m. coracobrachialis brevis (posterior portion); m. caudifemoralis brevis (ilium), m. pubotibialis), nearly isome at conditions were determined for elevation and depression of plesiosaur humerus and femur. If one would additionally consider protraction and retraction and long axis rotation of the humerus, muscle length changes would provide different results in all of these muscles. Possibly, these almost isometrical muscles had a complex muscle architecture (see Biewener & Roberts, 2000 for a review). Additionally, it is possible that m. triceps brachii and m. pubotibialis had long tendons (i.e., a large non-contractive component. Another possibility is that those muscles that lack length changes were actually reduced in plesiosaurs. Some clues might be given by the EPB: M. triceps brachii is much reduced or entirely reduced in Chelonioidea, depending on the species. The coracobrachialis brevis is markedly reduced in Size in Testudines (Walker, 1973). Possibly, the m. caudifemoralis brevis origin from the ilium was reduced in plesiosaurs and that m. caudifemoralis brevis arose only from the vertebral column. Musculus pubotibialis is absent in crocodilians (Otero, Gallina & Herrera, 2010; Suzuki et al., 2011).

Muscle length changes of agonistic and antagonistic muscles of the pelvic and pectoral girdle do not correspond well. On the one hand, this might be due to differences in the morphology and geometry of the pectoral and pelvic girdle. On the other hand, the resums could also change if flipper protraction and retraction were taken into account. Further, muscle architecture and tendon length were not and most probably cannot be inferred for extinct tetrapods.

759 Muscle forces

760 Humerus



On average, forces of muscles generated during the downstroke, i.e., by the humeral and femoral depressors and retractors, appear to have higher forces than muscles involved in the upstroke (Table 4; Tab 5). This could mean that in plesiosaurs the fore- and hindflipper downstroke was more efficient than the upstroke. Similarly, the foreflipper downstroke in Cheloniidae is more powerful than the upstroke (Davenport, Munks & Oxford, 1984; Krahl et al., 2019). However, this difference in efficiency is not found in all underwater fliers because it is not found in, e.g., penguins in which the foreflipper downstroke is as efficient as the upstroke (Clark & Bemis, 1979).

The way they were reconstructed here, the m. scapulohumeralis anterior and posterior appear to be solely humeral rotators because they operate with considerably high muscle forces during the downstroke (Table 4). This way, their elevational function is minor. This is surprising because in extant Lepidosauria both muscles are rather small (Jenkins & Goslow, 1983; Russell & Bauer, 2008). Either this implies that their origin and insertion areas were enlarged in Krahl (2020) or that m. scapulohumeralis anterior and posterior muscle forces would need testing with further FESA runs. These would show whether one can receive a similarly homogenous compressive stress distribution by reallocating a large portion of the muscle force to muscles with a similar function and LOA, e.g., m. latissimus dorsi, m. subcoracoscapularis, etc. LOAs of m. scapulohumeralis anterior and m. scapulohumeralis posterior which would wrap unusually around the dorsal tuberosity in posterior to anterior direction seem to underpin the hypothetical reallocation of muscle force to another muscle as aforementioned.

A surprising result is that m. pectoralis is the muscle that develops the highest muscle force during the foreflipper upstroke (Table 4), too. Although in total humeral elevators and protractors should be presumed to produce a higher power output, otherwise foreflipper elevation and protraction become impossible. Furthermore, the pectoral girdle is suspended from the vertebral column, the rib cage, and the gastralia by muscles and tendons (e.g. (Avery & Tanner, 1964; Walker, 1973). Recent studies have shown that a swinging pectoral and pelvic girdle can contribute substantially to locomotion in extant Otariinae, Testudines, and crocodylians (Walker, 1971a; Baier & Gatesy, 2013; Mayerl, Brainerd & Blob, 2016; Schmidt, Mehlhorn & Fischer, 2016). This indicates, that the importance of the contribution to locomotion of pectoral and pelvic girdle swinging in Tetrapoda is not only underestimated in extant taxa but surely in extinct taxa, too. An actively swinging pectoral and pelvic girdle could contribute to the range of motion of the plesiosaur fore- and hindflippers and to the total force with which the flippers are beaten. Especially in the plesiosaur shoulder region, where there is no bony or cartilaginous connection to the trunk (as opposed to the pelvic region), a strong shoulder musculature and ligaments connecting the pectoral girdle with the vertebral column, the ribs, and the gastralia would be necessary.

On the dorsal foreflipper m. extensor carpi ulnaris develops rather low muscle forces (1000 N) in comparison to m. extensor digitorum communis (6000 N). Musculus flexor carpi radialis and m. flexor digitorum longus are topologically comparably arranged to extensor carpi ulnaris and m. extensor digitorum communis but on the ventral side of the foreflipper.



 Contrastingly, m. flexor carpi radialis and m. flexor digitorum longus develop considerably lower muscle forces (both 1500 N) (Table 4). However, the extensor and flexor forces were only calculated based on their contribution to physiological loading of the femoral epicondyles. Extending the model by the digits could help to define them more precisely.

Femur

If one compares the muscle forces of the extensors and flexors of the plesiosaur humerus and femur, it becomes apparent that those of the femur (Table 5) are generally lower than those of the humerus (Table 4). This may be due to the fact that in the plesiosaur hindflipper, there are considerably more two-joint muscles and fewer as well as less independently operating extensors and flexors than in the foreflipper. The two-joint muscles aid in femur protraction/retraction, elevation/depression, and in knee flexion in extant Sauropsida (Snyder, 1954; Walker, 1973; Otero, Gallina & Herrera, 2010; Anzai et al., 2014), too. As the plesiosaur knee was immobile, these muscles were interpreted by Krahl (2020) to be part of the flipper long axis twisting mechanism additionally to their functions as depressors/elevators and protractors/retractors. Therefore, it is possible that the numerous two-joint muscles of the plesiosaur hindflipper partially aided in functions that were served by the much more differentiated extensors and flexors in the foreflipper (Krahl, 2020). Muscle forces of the two-joint muscles could not be determined in this study because they only indirectly influence FESA by adding to the counterforce imposed by the tibia and fibula. Therefore, it can be expected that the only extensor and the two flexors of the hindflipper should have in total lower muscle forces than the numerous extensors and flexors of the foreflipper. Finally, femur and humerus differ morphologically by the distal expansion, and possibly the hindflipper contributed less to propulsion than the foreflipper, as proposed by Lingham-Soliar (2000) and Liu et al. (2015).

Comparison to Cheloniidae humerus

There are some similarities in muscle forces of certain muscles in *Cryptoclidus eurymerus* (IGPB R 324) and in Cheloniidae: m. pectoralis develops the highest force of all muscles that insert proximally into the humerus (Krahl et al., 2019). Furthermore, of the main humeral elevators, m. subcoracoscapularis generates higher forces than m. latissimus dorsi in both taxa (Krahl et al., 2019). Musculus coracobrachialis brevis develops lower force in sea turtles (Krahl et al., 2019) than in plesiosaurs. Contrastingly, m. coracobrachialis longus develops higher forces in sea turtles (Krahl et al., 2019) than in plesiosaurs. While m. deltoideus scapularis and m. deltoideus clavicularis contribute in markedly different ways to propulsion in Cheloniidae (Krahl et al., 2019), they operate with broadly similar forces in plesiosaurs.

Another difference between the forces of humerus muscles of cheloniids (Krahl et al., 2019) and plesiosaurs is that in the former they vary by an order of magnitude unlike in the latter in which they do not necessarily differ much. These results support a hydrodynamic study of *Cryptoclidus eurymerus* (IGPB R 324) that finds flipper twisting to be crucial for underwater flight in plesiosaurs (Witzel, Krahl & Sander, 2015; Witzel, 2020). Furthermore, these findings



corroborate the myological flipper twisting mechanism proposed by (Krahl et al., 2019). Generally, higher muscle forces in plesiosaurs could be due to scaling effects.

The muscle bellies that produce these enormous muscle forces (up to 9600 N) in the shoulder girdle were large and took much space. Therefore, it is indeed-problematic that extensors and flexors proved to have produced similarly large forces because their potential origin surfaces are much smaller than for the glenoid spanning muscles. Different solutions to this paradox may exist. M. flexor digitorum longus, for instance, has a second head arising from the carpus in Sauropsida (Walker, 1973; Meers, 2003; Russell & Bauer, 2008), so it could have been able to develop substantially higher force, than just by the humeral muscle belly. Further, possibly these muscles have a complex architecture that saves space in comparison to the musculature originating from the pectoral girdle. Long tendinous structures could have been a mechanism to conserve energy during cruising (Roberts et al., 1997; Biewener & Roberts, 2000).

Dolphins have a relatively well ossified flipper skeleton, although there are basically no individual muscles identifiable anymore. They merely have layers of parallel fibred connective tissue covering the flipper bones (see Cooper et al., 2007, Figure 4, p. 1128). This means in reverse that the hydrodynamic forces plus the "muscle" force these layers of connective tissue can exert are in total enough to induce ossification of the flipper bones. Similar aponeurotic layerings, maybe also directed in the main directions of flipper twisting could account for a considerable part of the muscle forces calculated with FESA. Also, the connective tissue covering the broad space of the non-functional elbow joint, carpus, and manus could passively also conserve energy and thus passively compensate for some of the forces computed.

Conclusions

The highly aquatically adapted locomotor apparatus of plesiosaurs experienced little change throughout 135 Ma of plesiosaur evolution. The question of whether plesiosaurs rowed, flew underwater, or employed a combination of both has not been fully answered yet. Here we present a computer model which is in agreement with underwater flight in plesiosaurs based on comparative anatomical and muscle physiological data in accordance with mechanical principles. For this purpose, a foreflipper and hindflipper cast of IGPB R 324 were mounted on a wooden framework. With the help of screw eye pins, electrical terminal strips, and threads humerus and femur muscle LOA were recreated. Three positions representing maximum dorsal and ventral fore- and hindflipper excursion and a neutral position were fixed with ropes. For each muscle that spans glenoid and acetabulum muscle length was measured in all three positions. Then total muscle length changes over a flipper beat cycle were calculated for all muscles. A *Cryptoclidus* humerus and femur FE model were built from micro-CT scans of IGPB R 324. Then, FESA was conducted for load case downstroke and upstroke for both long bones. Muscle insertion angles were obtained from LOA recreation. Muscle forces were stochastically determined in iterative steps.

We demonstrate that by aiming at a homogenous compressive stress distribution in the humerus and femur of *Cryptoclidus* (IGPB R 324), it is possible to test muscle reconstructions



and their associated LOA with FESA. Muscle reconstructions by Krahl (2020) were found to be 881 882 largely corroborated, but they were also amended and corrected due to FESA. As in Cheloniidae, muscles wrapping around bony processes, i.e., the dorsal tuberosity of the plesiosaur humerus 883 and dorsal trochanter of the plesiosaur femur, as well as their epicondyles, proved to be 884 885 necessary to load the aforementioned structures. Further, measuring the total length changes of all muscles that insert into, originate from, and span humerus and femur of a plesiosaur showed 886 that a m. deltoideus scapularis origin from the lateral scapula is unphysiological. This infers a 887 reduction of this muscle from this part of its origin site which is well supported across 888 Sauropsida (Walker, 1973; Meers, 2003; Russell & Bauer, 2008). Muscle forces show some 889 correlation with cheloniid humerus musculature but also differences which underlines that 890 underwater flight in both lineages was achieved in convergent ways. High extensor and flexor 891 forces in plesiosaurs corroborate the hypothesis that flipper long axis twisting was essential for 892 plesiosaur underwater flight. 893

894 895

896

897

898 899

900

901

902

Acknowledgements

We are grateful to Aart Walen (Creatures and Features), Arnhem, The Netherlands, for kindly providing a cast of the pectoral and pelvic girdle and foreflipper and hindflipper of IGPB R 324 that was crucial to this study. The authors greatly appreciate the help of L. Baumeister of the Biomechanics Research Group, Chair of Product Development, Faculty of Mechanical Engineering, Ruhr-University Bochum, Germany, with FE models of the femur. The authors thank Tanja Wintrich (Bonn) for producing the micro-CT scans of the humerus and femur of IGPB R 324. This study was funded by Deutsche Forschungsgemeinschaft (DFG) grant WI1389/8-1.

903904905

References

- Alexander RM, Vernon A. 1975. The dimensions of knee and ankle muscles and the forces they exert. *Journal of Human Movement Studies* 1:115–123.
- 908 Allen V, Elsey RM, Jones N, Wright J, Hutchinson JR. 2010. Functional specialization and ontogenetic scaling of limb anatomy in *Alligator mississippiensis*. *Journal of Anatomy* 216
- **910 (4)**:423–445.
- 911 Anapol F, Barry K. 1996. Fibre architecture of the extensors of the hindlimb in semiterrestrial
- and arboreal guenons. *American Journal of Physical Anthropology* **99**:429-447.a.
- 913 Andrews CW. 1910. A Descriptive Catalogue of the Marine Reptiles of the Oxford Clay, Part I.
- 914 London, UK: British Museum (Natural History).
- 915 Anzai W, Omura A, Diaz AC, Kawata M, Endo H. 2014. Functional morphology and
- 916 comparative anatomy of appendicular musculature in Cuban *Anolis* lizards with different
- 917 locomotor habits. *Zoological Science* **31 (7)**:454–463.
- 918 Araújo R, Correia F. 2015. Soft-tissue anatomy of the plesiosaur pectoral girdle inferred from
- basal Eosauropterygia taxa and the extant phylogenetic bracket. *Palaeontologia Electronica* **18**
- 920 (1):1–32.



- 921 Araújo R, Polcyn MJ, Schulp AS, Mateus O, Jacobs LL, Gonçalves AO, Morais M-L. 2015.
- 922 A new elasmosaurid from the early Maastrichtian of Angola and the implications of girdle
- 923 morphology on swimming style in plesiosaurs. *Netherlands Journal of Geosciences Geologie*
- 924 *en Mijnbouw* **94 (1)**:109–120.
- 925 Avery, F D, Tanner WW. 1964. The osteology and myology of the head and thorax regions of
- 926 the obesus group of the genus Sauromalus dumeril (Iguanidae). Brigham Young University
- 927 Science Bulletin, Biological Series 5 (3):1–30.
- 928 Azizi E, Brainerd EL, Roberts TJ. 2008. Variable gearing in pennate muscles. *Proceedings of*
- 929 the National Academy of Sciences of the United States of America 105 (5):1745–1750.
- 930 Baier DB, Gatesy SM. 2013. Three-dimensional skeletal kinematics of the shoulder girdle and
- 931 forelimb in walking *Alligator*. *Journal of Anatomy* **223** (5):462–473.
- 932 **Bardet N. 1994.** Extinction events among Mesozoic marine reptiles. *Historical Biology* 7
- **933 (4)**:313–324.
- 934 Bardet N, Falconnet J, Fischer V, Houssaye A, Jouve S, Pereda Suberbiola X, Pérez-García
- 935 A, Rage J-C, Vincent P. 2014. Mesozoic marine reptile palaeobiogeography in response to
- 936 drifting plates. Gondwana Research 26 (3–4):869–887.
- 937 **Baudinette RV, Gill P. 1985.** The energetics of 'flying' and 'paddling' in water: Locomotion in
- penguins and ducks. *Journal of Comparative Physiology B* **155** (3):373–380.
- 939 Biewener AA, Corning WR, Tobalske BW. 1998. In vivo pectoralis muscle force-length
- 940 behavior during level flight in pigeons (Columba livia). Journal of Experimental Biology 201
- 941 (24):3293–3307.
- 942 **Biewener AA, Dial KP. 1995.** In vivo strain in the humerus of pigeons (*Cloumba livia*) during
- 943 flight. *Journal of Morphology* **225**:61–65.
- 944 Biewener AA, Konieczynski DD, Baudinette RV. 1998. In vivo muscle force-length behavior
- 945 during steady-speed hopping in tammar wallabies. *Journal of Experimental Biology* **201**
- **946 (11)**:1681–1694.
- 947 **Biewener AA, Roberts TJ. 2000.** Muscle and tendon contributions to force, work, and elastic
- energy savings: A comparative perspective. Exercise and Sport Sciences Reviews 28 (3):99–107.
- 949 **Blob RW, Biewener AA. 1999.** In vivo locomotor strain in the hindlimb bones of *Alligator*
- 950 mississpiensis and Iguana iguana: Implications for the evolution of limb bone safety factor and
- 951 non-sprawling limb posture. *Journal of Experimental Biology* **202**:1023–1046.
- 952 Bryant HN, Russel AP. 1992. The role of phylogenetic analysis in the inference of unpreserved
- 953 attributes of extinct taxa. Philosophical Transactions of the Royal Society London B 337:405–
- 954 418.
- 955 Burkholder TJ, Fingado B, Bron S, Lieber R. 1994. Relationship between muscle fiber types
- 956 and sizes and muscle architectural properties in the mouse hindlimb. *Journal of Morphology*
- 957 **221**:177–199.
- 958 **Butcher MT, Blob RW. 2008.** Mechanics of limb bone loading during terrestrial locomotion in
- 959 river cooter turtles (*Pseudemys concinna*). Journal of Experimental Biology **211 (8)**:1187–1202.



- 960 Butcher MT, Espinoza NR, Cirilo SR, Blob RW. 2008. In vivo strains in the femur of river
- 961 cooter turtles (*Pseudemys concinna*) during terrestrial locomotion: Tests of force-platform
- models of loading mechanics. *Journal of Experimental Biology* **211** (15):2397–2407.
- 963 Caldwell MW. 1997. Limb osteology and ossification patterns in *Cryptoclidus* (Reptilia:
- 964 Plesiosauroidea) with a review of Sauropterygian limbs. *Journal of Vertebrate Paleontology* 17
- **965 (2)**:295–307.
- 966 Carpenter K, Sanders F, Reed B, Reed J, Larson P. 2010. Plesiosaur swimming as interpreted
- 967 from skeletal analysis and experimental results. *Transactions of the Kansas Academy of Science*
- 968 **113 (1/2)**:1–34.
- 969 Carrano MT. 1998. Locomotion in non-avian dinosaurs: Integrating data from hindlimb
- 970 kinematics, in vivo strains, and bone morphology. *Paleobiology* **24** (**04**):450–469.
- 971 Carter DR, Orr TE, Fyhrie DP. 1989. Relationships between loading history and femoral
- 972 cancellous bone architecture. *Journal of Biomechanics* **22** (3):231–244.
- 973 Clark BD, Bemis W. 1979. Kinematics of swimming of penguins at the Detroit Zoo. *Journal of*
- 974 Zoology **188** (3):411–428.
- 975 Cooper LN, Dawson SD, Reidenberg JS, Berta A. 2007. Neuromuscular anatomy and
- evolution of the cetacean forelimb. *The Anatomical Record* **290** (9):1121–1137.
- 977 Curtis N, Witzel U, Fitton L, O'Higgins P, Fagan MJ. 2011. The mechanical significance of
- 978 the temporal fasciae in *Macaca fascicularis*: An investigation using finite element analysis. *The*
- 979 *Anatomical Record* **294 (7)**:1178–1190.
- 980 Davenport J, Munks SA, Oxford PJ. 1984. A comparison of the swimming of marine and
- 981 freshwater turtles. *Proceedings of the Royal Society B: Biological Sciences* **220** (1221):447–475.
- 982 Elliott KH, Ricklefs RE, Gaston AJ, Hatch SA, Speakman JR, Davoren GK. 2013. High
- 983 flight costs, but low dive costs, in auks support the biomechanical hypothesis for flightlessness in
- 984 penguins. Proceedings of the National Academy of Sciences of the United States of America 110
- 985 **(23)**:9380–9384.
- 986 **English AWM. 1977.** Structural correlates of forelimb function in fur seals and sea lions.
- 987 *Journal of Morphology* **151 (3)**:325–352.
- 988 **Feldkamp SD. 1987.** Foreflipper propulsion in the California sea lion, *Zalophus californianus*.
- 989 *Journal of Zoology* **212**:43–57.
- 990 **Felsenthal N, Zelzer E. 2017.** Mechanical regulation of musculoskeletal system development.
- 991 Development **144 (23)**:4271–4283.
- 992 **Fish FE. 1996.** Transitions from drag-based to lift-based propulsion in mammalian swimming.
- 993 *American Zoologist* **36 (6)**:628–641.
- 994 **Fish FE. 2002.** Balancing requirements for stability and maneuverability in cetaceans.
- 995 *Integrative and Comparative Biology* **42**:85–93.
- 996 Fish FE. 2004. Structure and mechanics of nonpiscine control surfaces. *IEEE Journal of*
- 997 *Oceanic Engineering* **29 (3)**:605–621.
- 998 Fish FE, Battle JM. 1995. Hydrodynamic design of the humpback whale flipper. *Journal of*
- 999 *Morphology* **225** (1):51–60.



- 1000 Frey E, Riess J. 1982. Considerations concerning plesiosaur locomotion. Neues Jahrbuch für
- 1001 Geologie und Paläontologie, Abhandlungen **164**:193–194.
- 1002 Gans C. 1982. Fibre architecture and muscle function. Exercise and Sport Science Reviews 10
- 1003 (1):160–207.
- 1004 Godfrey SJ. 1984. Plesiosaur subaqueous locomotion: a reappraisal. Neues Jahrbuch für
- 1005 Geologie und Palaontologie Monatshefte:661–672.
- 1006 Großmann F. 2006. Taxonomy, phylogeny and palaeoecology of the plesiosauroids
- 1007 (Sauropterygia, Reptilia) from the Posidonia shale (Toarcian, Lower Jurassic) of Holzmaden,
- 1008 south west Germany. Dissertation, Eberhard-Karls-Universität.
- 1009 Huq E, Wall CE, Taylor AB. 2015. Epaxial muscle fiber architecture favors enhanced
- 1010 excursion and power in the leaper *Galago senegalensis*. *Journal of Anatomy*.
- 1011 **Jenkins FA, Goslow GE. 1983.** The functional anatomy of the shoulder of the savannah monitor
- 1012 lizard (Varanus exanthematicus). Journal of Morphology 175:195–216.
- 1013 Klenner S, Witzel U, Paris F, Distler C. 2015. Structure and function of the septum nasi and
- the underlying tension chord in crocodylians. *Journal of Anatomy* **228** (1):113–124.
- 1015 **Krahl A. 2020.** Underwater flight in sea turtles and plesiosaurs Dissection, muscle
- 1016 reconstructions, analog models, and finite element structure analyses inform on flipper twisting
- and muscle forces in plesiosaurs. PhD-dissertation, Mathematisch-Naturwissenschaftliche
- 1018 Fakultät der Rheinischen Friedrich-Wilhelms-Universität Bonn, Bonn. p.311. https://nbn-
- 1019 resolving.org/urn:nbn:de:hbz:5-59143.
- 1020 Krahl A, Lipphaus A, Witzel U, Sander PM, Maffucci F, Hochscheid S. 2019. Humerus
- osteology, myology, and finite element structure analysis of Cheloniidae. *The Anatomical*
- 1022 Record 303 (8): 2177-2191. https://doi.org/10.1002/ar.24311.
- 1023
- 1024 **Kummer B. 2005.** *Biomechanik.* Köln: Deutscher Ärzte Verlag.
- 1025 Lieberman DE, Polk JD, Demes B. 2004. Predicting long bone loading from cross-sectional
- 1026 geometry. American Journal of Physical Anthropology 123 (2):156–171.
- 1027 **Lingham-Soliar T. 2000.** Plesiosaur locomotion: Is the four-wing problem real or merely an
- 1028 atheoretical exercise? Neues Jahrbuch für Geologie und Paläontologie, Abhandlungen 217
- 1029 (1):45–87.
- 1030 Lipphaus A, Witzel U. 2018. Biomechanical study of the development of long bones: Finite
- 1031 element structure synthesis of the human second proximal phalanx under growth conditions. *The*
- 1032 Anatomical Record.
- 1033 Liu S, Smith AS, Gu Y, Tan J, Liu CK, Turk G. 2015. Computer simulations imply forelimb-
- dominated underwater flight in plesiosaurs. *PLoS Computational Biology* **11 (12)**:e1004605.
- 1035 **Louw GJ. 1992.** Functional anatomy of the penguin flipper. *Journal of the South African*
- 1036 *Veterinary Association* **63 (3)**:113–120.
- 1037 Lutz F, Mastel R, Runge M, Stief F, Schmidt A, Meurer A, Witte H. 2016. Calculation of
- 1038 muscle forces during normal gait under consideration of femoral bending moments. *Medical*
- 1039 Engineering & Physics **38** (9):1008–1015.



- 1040 Main RP, Biewener AA. 2004. Ontogenetic patterns of limb loading, in vivo bone strains and
- growth in the goat radius. *The Journal of Experimental Biology* **207** (15):2577–2588.
- 1042 Main RP, Biewener AA. 2007. Skeletal strain patterns and growth in the emu hindlimb during
- ontogeny. The Journal of Experimental Biology 210 (15):2676–2690.
- 1044 Mayerl CJ, Brainerd EL, Blob RW. 2016. Pelvic girdle mobility of cryptodire and pleurodire
- turtles during walking and swimming. *The Journal of Experimental Biology* **219** (Pt 17):2650–
- 1046 2658.
- 1047 McCabe K, Henderson K, Pantinople J, Richards HL, Milne N. 2017. Curvature reduces
- bending strains in the quokka femur. *PeerJ* **5**:e3100.
- 1049 Meers MB. 2003. Crocodylian forelimb musculature and its relevance to Archosauria. *The*
- 1050 *Anatomical Record* **274 (2)**:891–916.
- 1051 Merck JW. 1997. A phylogenetic analysis of the euryapsid reptiles. *Journal of Vertebrate*
- 1052 *Paleontology* **17**:65.
- 1053 Milne N. 2016. Curved bones: An adaptation to habitual loading. *Journal of Theoretical Biology*
- **1054 407**:18–24.
- 1055 Motani R. 2009. The evolution of marine reptiles. Evolution: Education and Outreach 2
- **1056 (2)**:224–235.
- 1057 Muscutt LE, Dyke G, Weymouth GD, Naish D, Palmer C, Ganapathisubramani B. 2017.
- 1058 The four-flipper swimming method of plesiosaurs enabled efficient and effective locomotion.
- 1059 Proceedings of the Royal Society B: Biological Sciences) **284 (1861)**:20170951.
- 1060 Narici MV, Landoni L, Minetti AE. 1992. Assessment of human knee extensor muscles stress
- 1061 from in vivo physiological cross-sectional area and strength measurements. European Journal of
- 1062 Applied Physiology and Occupational Physiology 65 (5):438–444.
- Neenan JM, Klein N, Scheyer TM. 2013. European origin of placodont marine reptiles and the
- evolution of crushing dentition in Placodontia. *Nature Communications* **4**:1621.
- 1065 Otero A, Gallina PA, Herrera Y. 2010. Pelvic musculature and function of *Caiman latirostris*.
- 1066 *Herpetological Journal* **20**:173–184.
- 1067 Pace CM, Blob RW, Westneat MW. 2001. Comparative kinematics of the forelimb during
- 1068 swimming in red-eared slider (*Trachemys scripta*) and spiny softshell (*Apalone spinifera*) turtles.
- 1069 The Journal of Experimental Biology **204**:3261–3271.
- 1070 Pinshow B, Fedak MA, Schmidt-Nielsen K. 1977. Terrestrial locomotion in penguins: It costs
- 1071 more to waddle. *Science* **195** (**4278**):592–594.
- 1072 Powell PL, Roy RR, Kanim P, Bello MA, Edgerton VR. 1984. Predictability of skeletal
- 1073 muscle tension from architectural determinations in guinea pig hindlimbs. *Journal of Applied*
- 1074 *Physiology* **57 (6)**:1715–1721.
- 1075 Rassier DE, MacIntosh BR, Herzog W. 1999. Length dependence of active force production in
- skeletal muscle. *Journal of Applied Physiology* **86 (5)**:1445–1457.
- 1077 Rayfield EJ. 2007. Finite element analysis and understanding the biomechanics and evolution of
- 1078 living and fossil organisms. Annual Review of Earth and Planetary Sciences 35 (1):541–576.



- 1079 Rhodin AGJ, Ogden JA, Conlogue GJ. 1981. Chondro-osseous morphology of *Dermochelys*
- 1080 *coriacea*, a marine reptile with mammalian skeletal features. *Nature* **290**:244.
- 1081 **Rieppel O, Reisz RR. 1999.** The origin and early evolution of turtles. *Annual Review of Ecology*
- 1082 *and Systematics* **30**:1–22.
- 1083 Rivera ARV, Rivera G, Blob RW. 2013. Forelimb kinematics during swimming in the pig-
- nosed turtle, Carettochelys insculpta, compared with other turtle taxa: Rowing versus flapping,
- 1085 convergence versus intermediacy. The Journal of Experimental Biology 216 (Pt 4):668–680.
- 1086 Rivera ARV, Wyneken J, Blob RW. 2011. Forelimb kinematics and motor patterns of
- swimming loggerhead sea turtles (*Caretta caretta*): Are motor patterns conserved in the
- evolution of new locomotor strategies? *The Journal of Experimental Biology* **214 (19)**:3314–
- 1089 3323.
- 1090 Rivera G, Rivera ARV, Blob RW. 2011. Hydrodynamic stability of the painted turtle
- 1091 (*Chrysemys picta*): Effects of four-limbed rowing versus forelimb flapping in rigid-bodied
- tetrapods. The Journal of Experimental Biology 214 (Pt 7):1153–1162.
- 1093 Roberts TJ, Marsh RL, Weyand PG, Taylor CR. 1997. Muscular force in running turkeys:
- 1094 The economy of minimizing work. *Science* **275** (5303):1113–1115.
- 1095 **Robinson JA. 1975.** The locomotion of plesiosaurs. *Neues Jahrbuch für Geologie und*
- 1096 Paläontologie, Abhandlungen 149:286–332.
- 1097 **Robinson JA. 1977.** Intracorporal force transmission in plesiosaurs. *Neues Jahrbuch Geologie*
- 1098 Paläontologie, Abhandlungen 153:86–128.
- 1099 Russell AP, Bauer AM. 2008. The appendicular locomotor apparatus of Sphenodon and normal-
- 1100 limbed squamates. In: Gans C, Parsons TS, editors. *Biology of the Reptilia* Volume 21 New
- 1101 York: Academic Press. 1–465.
- 1102 Sachs S, Hornung JJ, Kear BP. 2016. Reappraisal of Europe's most complete Early Cretaceous
- 1103 plesiosaurian: Brancasaurus brancai Wegner, 1914 from the "Wealden facies" of Germany.
- 1104 *PeerJ* **4**:e2813.
- 1105 Sacks RD, Roy RR. 1982. Architecture of the hind limb muscles of cats: Functional
- 1106 significance. *Journal of Morphology* **173 (2)**:185–195.
- 1107 Schmidt M, Mehlhorn M, Fischer MS. 2016. Shoulder girdle rotation, forelimb movement and
- 1108 the influence of carapace shape on locomotion in *Testudo hermanni* (Testudinidae). *The Journal*
- 1109 of Experimental Biology **219 (Pt 17)**:2693–2703.
- 1110 **Schreiweis DO. 1982.** A comparative study of the appendicular musculature of penguins (Aves:
- 1111 Sphenisciformes). *Smithsonian Contributions to Zoology* **341**:1–46.
- 1112 Sheffield KM, Butcher MT, Shugart SK, Gander JC, Blob RW. 2011. Locomotor loading
- 1113 mechanics in the hindlimbs of tegu lizards (*Tupinambis merianae*): Comparative and
- 1114 evolutionary implications. *The Journal of Experimental Biology* **214** (15):2616–2630.
- 1115 **Shufeldt RW. 1901.** Osteology of the penguins. *Journal of Anatomy and Physiology* **35 (3)**:390–
- 1116 405.



- 1117 Snover ML, Rhodin AGJ. 2008. Comparative ontogenetic and phylogenetic aspects of
- 1118 chelonian chondro-osseous growth and skeletochronology. In: Wyneken J, Godfrey MH, Bels V,
- eds. *Biology of Turtles*. Boca Raton, Florida, USA: CRC Press, 17–43.
- 1120 Snyder RC. 1954. The anatomy and function of the pelvic girdle and hindlimb in lizard
- 1121 locomotion. *The American Journal of Anatomy* **95** (1):1–45.
- 1122 Sues H-D. 1987. Postcranial skeleton of *Pistosaurus* and interrelationships of the Sauropterygia
- 1123 (Diapsida). Zoological Journal of the Linnean Society 90:109–131.
- 1124 Suzuki D, Chiba K, Tanaka Y, Hayashi S. 2011. Myology of crocodiles III: Pelvic girdle and
- hindlimb. Fossils The Palaeontological Society of Japan **90**:37–60.
- 1126 Suzuki D, Hayashi S. 2010. Myology of crocodiles II: Pectoral girdle and forelimb. Fossils The
- 1127 Palaeontological Society of Japan 87:83–102.
- 1128 Sverdlova NS, Witzel U. 2010. Principles of determination and verification of muscle forces in
- the human musculoskeletal system: Muscle forces to minimise bending stress. *Journal of*
- 1130 *Biomechanics* **43 (3)**:387–396.
- **Tarlo LB. 1958.** The scapula of *Pliosaurus macromerus* Phillips. *Palaeontology* 1:193–199.
- 1132 Tarsitano S, Riess J. 1982. Plesiosaur locomotion: Underwater flight versus rowing. *Neues*
- 1133 *Jahrbuch für Geologie und Paläontologie, Abhandlungen* **164**:188–192.
- 1134 **Taylor MA. 1989.** Sea-saurians for sceptics. *Nature* **338** (6217):625–626.
- 1135 Vincent P, Bardet N, Houssaye A, Amaghzaz M, Meslouh S. 2013. New plesiosaur specimens
- 1136 from the Maastrichtian phosphates of Morocco and their implications for the ecology of the latest
- 1137 Cretaceous marine apex predators. *Gondwana Research* **24 (2)**:796–805.
- 1138 Vincent P, Bardet N, Pereda Suberbiola X, Bouya B, Amaghzaz M, Meslouh S. 2011.
- 1139 Zarafasaura oceanis, a new elasmosaurid (Reptilia: Sauropterygia) from the Maastrichtian
- Phosphates of Morocco and the palaeobiogeography of latest Cretaceous plesiosaurs. *Gondwana*
- 1141 *Research* **19 (4)**:1062–1073.
- 1142 Walker JA, Westneat MW. 2000. Mechanical performance of aquatic rowing and flying.
- 1143 Proceedings of the Royal Society of London B: Biological Sciences 267 (1455):1875–1881.
- 1144 Walker WF. 1971a. A structural and functional analysis of walking in the turtle, *Chrysemys*
- 1145 picta marginata. Journal of Morphology 134 (2):195–214.
- 1146 Walker WF. 1971b. Swimming in sea turtles of the family Cheloniidae. *Copeia* 1971:229–233.
- 1147 Walker WF. 1973. The locomotor apparatus of Testudines. In: Gans C, Parsons TS, editors.
- 1148 *Biology of Reptilia* Volume 4. New York: Academic Press.1–100.
- 1149 Watson DMS. 1924. The elasmosaurid shoulder-girdle and fore-limb. *Proceedings of the*
- 1150 Zoological Society of London **58**:885–917.
- 1151 Williamson MR, Dial KP, Biewener AA. 2001. Pectoralis muscle performance during
- ascending and slow level flight in mallards (Anas platyrhynchos). Journal of Experimental
- 1153 *Biology* **204 (3)**:495–507.
- 1154 Williston SW. 1914. Water reptiles of the past and present. Chicago, USA: University of
- 1155 Chicago Press.



- 1156 Wintrich T, Hayashi S, Houssaye A, Nakajima Y, Sander PM. 2017. A Triassic plesiosaur
- skeleton and bone histology inform on evolution of a unique body plan. Science Advances 3
- 1158 **(12)**:e1701144.
- 1159 Wittmer LM. 1995. The Extant Phylogenetic Bracket and the importance of reconstructing soft
- 1160 tissues in fossils. In: Thomason JJ, ed. Functional Morphology in Vertebrate Paleontology. New
- 1161 York: Cambridge University Press, 19–33.
- 1162 Witzel, U. 2020. Funktionsmorphologische Forschung mit Hilfe biomechanischer Ansätze im
- 1163 Rahmen der Phylogenie und ontogenetischen Entwicklung zum Vertebraten. In: Werneburg I,
- 1164 Betz O, eds. Phylogenie, Funktionsmorphologie und Bionik Schriften zum 60.
- 1165 Phylogenetischen Symposium in Tübingen. Tübingen, Germany: Scidinge Hall Verlag, 187-220.
- 1166 Witzel U, Mannhardt J, Goessling R, Micheli Pd, Preuschoft H. 2011. Finite element
- analyses and virtual syntheses of biological structures and their application to sauropod skulls.
- 1168 In: Klein, N., Remes, K., Gee, C. T., & Sander, P. M., ed. Biology of the Sauropod Dinosaurs:
- 1169 *Understanding the Life of Giants*, 171–182.
- 1170 Witzel U, Preuschoft H. 2005. Finite-element model construction for the virtual synthesis of the
- skulls in vertebrates: Case study of *Diplodocus*. The Anatomical Record **283** (2):391–401.
- 1172 Witzel U, Krahl A, Sander PM. 2015. Hydrodynamische Untersuchung des Schimmvorgangs
- 1173 eines jurassischen Plesiosauriers: Bestimmung des Körperwiderstands und der Vortriebskräfte
- 1174 der Flossen. ZfB-Scriptum Veröffentlichungen des Zentrums für Biodokumentation (ZfB) 4 (58).
- 1175 Woodward BL, Winn JP, Fish FE. 2006. Morphological specializations of baleen whales
- associated with hydrodynamic performance and ecological niche. *Journal of Morphology* **267**
- **1177 (11)**:1284–1294.
- 1178 Wyneken J. 1997. Sea turtle locomotion: Mechanisms, behavior, and energetics. In: Lutz PL,
- 1179 Musick JA, eds. *The Biology of Sea Turtles*. Boca Raton, Florida, USA: CRC Press, 165–198.
- 1180 Young VKH, Blob RW. 2015. Limb bone loading in swimming turtles: Changes in loading
- facilitate transitions from tubular to flipper-shaped limbs during aquatic invasions. *Biology*
- 1182 *Letters* **11 (6)**:20150110.
- 1183 Young VKH, Wienands CE, Wilburn BP, Blob RW. 2017. Humeral loads during swimming
- and walking in turtles: Implications for morphological change during aquatic reinvasions. *The*
- 1185 *Journal of Experimental Biology* **220 (21)**:3873–3877.
- 1186 **Zug GR. 1971.** Buoyancy, locomotion, morphology of the pelvic girdle and hindlimb, and
- 1187 systematics of cryptodiran turtles: University of Michigan Museum of Zoology.



Table 1(on next page)

Changes in length of *Cryptoclidus eurymerus* (IGPB R 324) humerus and femur muscles



Musculus	number	maximu	neutral	maximu	muscle length	muscle length	muscle length	muscle length	muscle	muscle	total length
	coding for	m	positio	m dorsal	change (-=	change (-=	change (-=	change (-=	stretching =	contraction =	change of
	muscle	ventral	n [cm]	excursio	shortening, +	shortening, +	shortening, +	shortening, +	muscle neutral	muscle neutral	muscle [%] (=
	(portion)	excursio		n [cm]	=	= lengthening)	= lengthening)	= lengthening)	position	position	muscle
	in	n [cm]			lengthening)	from neutral	from neutral	from neutral	(=100%) +	(=100%) -	stretching -
	respective				from neutral	position to	position to	position to	muscle	shortening of	muscle
	diagram				position to	maximum	maximum	maximum	lengthening [%]	muscle [%]	contraction)
					maximum	ventral	dorsal	dorsal			,
					ventral	excursion [%]	excursion	excursion [%]			
					excursion		[cm]				
					[cm]		,				
m. deltoideus	1	22,2	13,6	9,8	8,6	63,24	-3,8	-7,63	163,24	92, 37	70,87
scapularis											
m. deltoideus	2	22,6	22,6	22,6	0	0	0	0	100	100	0
scapularis											
corrected											
m. deltoideus	3	36,5	36,5	36,5	0	0	0	0	100	100	0
clavicularis											
m. latissimus	4	42,7	34,9	29,8	7,8	22,35	-5,1	-14,61	122,35	85,39	36,96
dorsi (anterior)											
m. latissimus	5	43,9	37,6	32,6	6,3	16,76	-5	-13,3	116,76	86,7	30,06
dorsi (in											
between)											
m. latissimus	6	52,7	47,9	42,2	4,8	10,02	-5,7	-11,9	110,02	88,1	21,92
dorsi (posterior)											
m.	7	32,8	29,3	24,3	3,5	11,95	-5	-17,06	111,95	82,94	29,01
subcoracoscapula											
ris (anterior											
portion)											
m.	8	36,3	33,2	33,2	3,1	9,34	0	0	109,34	100	9,34
subcoracoscapula											
ris (posterior											
portion)											

m.	9	30,9	29,5	27,4	1,4	4,75	-2,1	-7,12	104,75	92,88	11,87
scapulohumeralis											
anterior											
m.	10	24,9	22,7	19,4	2,2	9,69	-3,3	-14,54	109,69	85,46	24,23
scapulohumeralis posterior											
m. coracobrachialis brevis (anterior)	11	29,3	36,7	40,5	-7,4	-20,16	3,8	10,35	110,35	79,84	30,51
m.	12	43,8	43,8	45,5	0	0	1,7	3,88	103,88	100	3,88
coracobrachialis											
brevis (posterior)											
m. coracobrachialis	13	43,1	52	53,9	-8,9	-17,12	1,9	3,65	103,65	82,88	20,77
longus m. pectoralis	14	29,9	30,4	35,6	-0,5	-1,64	5,2	17,11	117, 11	98,36	18,75
(anterior)	14	29,9	30,4	33,0	-0,3	-1,04	3,2	17,11	117, 11	98,30	16,73
m. pectoralis (posterior)	15	27,4	33,1	39,2	-5,7	-17,22	6,1	18,43	118,43	82,78	35,65
m. supracoracoideus	16	24,5	31,7	31,7	-7,2	-22,71	0	0	100	77,29	22,71
m. biceps brachii	17	56,7	67,8	72,4	-11,1	-16,37	4,6	6,78	106,78	83,63	23,15
m. triceps brachii (anterior)	18	36,8	36,8	36,8	0	0	0	0	100	100	0
m. triceps brachii (posterior)	19	31,2	31,2	31,2	0	0	0	0	100	100	0

1

Musculus	number	maximum	neutral	maximum	muscle length	muscle length	muscle length	muscle length	muscle	muscle	total length
	coding for	ventral	position	dorsal	change (-=	change (-=	change (-=	change (-=	stretching =	contraction =	change of
	muscle	excursion	[cm]	excursion	shortening, +	shortening, +=	shortening, +=	shortening, +=	muscle neutral	muscle neutral	muscle [%] (=
	(portion) in	[cm]		[cm]	=	lengthening)	lengthening)	lengthening)	position	position (=100%)	muscle
	respective				lengthening)	from neutral	from neutral	from neutral	(=100%) +	- shortening of	stretching -



	diagram				from neutral	position to	position to	position to	muscle	muscle [%]	muscle
					position to	maximum	maximum	maximum	lengthening [%]		contraction)
					maximum	ventral	dorsal excursion	dorsal excursion			
					ventral	excursion [%]	[cm]	[%]			
					excursion						
					[cm]						
m. caudofemoralis	1	61,3	63,5	64,6	-2,2	-3,46	1,1	6,15	106,15	96,54	9,61
longus											
m. caudofemoralis	2	17,9	17,9	17,9	0	0	0	0	100	100	0
brevis (ilium)											
m. caudofemoralis	3	37,6	36,9	33,6	0,7	1,9	-3,3	-8,94	101,9	96,7	5,2
brevis (vc)											
m. flexor tibialis	4	63,7	58,4	52,3	5,3	9,8	-6,1	-10,45	109,8	93,9	15,9
internus (vc)											
m. flexor tibialis	5	43,1	47,1	49,2	-4	-8,49	2,1	4,46	104,46	91,51	12,95
internus (ischium)											
m. flexor tibialis	6	42,8	47,5	49,4	-4,7	-9,89	1,9	4	104	90,11	13,89
externus (ischium)											
m. flexor tibialis	7	42,6	37,2	31,9	5,4	14,52	-5,3	-14,25	114,52	85,75	28,77
externus (ilium)											
m. iliofibularis	8	33,1	29	25,3	4,1	14,13	-3,7	-12,76	114,13	87,24	26,89
m. ambiens	9	29,3	29,3	31,7	0	0	2,4	8,19	108,19	100	8,19
m.	10	38,3	42,3	45,8	-4	-9,46	3,5	8,27	108,27	90,54	17,73
puboischiotibialis											
m. pubotibialis	11	33,4	33,4	33,4	0	0	0	0	100	100	0
m. iliofemoralis	12	18,3	14,2	13,6	4,1	28,87	-0,6	-4,23	128,87	95,77	33,1
m.	13	21,5	21,5	23,7	0	0	2,2	10,23	110,23	100	10,32
ischiotrochantericus											
m. iliotibialis	14	40,1	26,6	26,6	7,3	27,44	0	0	127,44	100	27,44
m. adductor femoris	15	30,4	32,8	36,2	-2,4	-7,31	3,4	6,71	106,71	92,69	14,02
(anterior)											

m. adductor femoris	16	26,6	30	32,9	-3,4	-11,33	2,9	9,67	109,67	88,67	21
(lateroposterior)											
m.	17	36,8	32,3	30,3	4,5	14,85	-2	-6,19	114,85	93,81	21,04
puboischiofemoralis											
internus (pubis)											
m.	18	29,4	27,2	23,3	2,2	8,09	-3,9	-14,34	108,09	85,66	22,43
puboischiofemoralis											
internus (ischium)											
m.	19	10,4	9,5	9,5	0,9	9,47	0	0	109,47	100	9,47
puboischiofemoralis											
internus (ilium)											
m.	20	39,6	32,1	28,1	7,5	23,36	-4	-12,46	123,36	87,54	35,82
puboischiofemoralis											
internus (vertebral											
column)											
m.	21	39,1	42,5	45,7	-3,4	-8	3,2	7,5	107,5	92	15,5
puboischiofemoralis											
externus (pubis)											
m.	22	22,9	27,6	29,4	-4,7	-17,03	1,8	6,52	106,52	82,97	23,55
puboischiofemoralis											
externus (ischium)											



Table 2(on next page)

Agonistic and antagonistic humerus muscles of Cryptoclidus eurymerus (IGPB R 324)



agonists	antagonists
anterior portion of m. latissimus dorsi	posterior portion m. pectoralis (depression
(eventually m. scapulohumeralis posterior	and retraction)
and m. scapulohumeralis anterior)	
(elevation, protraction)	
posterior portion of m. latissimus dorsi	anterior portion of m. pectoralis
(elevation, retraction)	(protraction, depression)
m. subcoracoscapularis (anterior portion),	m. coracobrachialis longus, m.
m. deltoideus scapularis (both elevation,	coracobrachialis brevis, m. biceps, posterior
protraction)	portion of m. supracoracoideus (all
	retraction, depression)
m. subcoracoscapularis (posterior portion)	anterior portion of m. supracoracoideus, m.
(elevation, retraction)	deltoideus clavicularis (all depression,
	protraction)
m. latissimus dorsi, anterior portion of m.	m. scapulohumeralis anterior, m.
pectoralis, posterior portion of m.	scapulohumeralis posterior, anterior portion
subcoracoscapularis, m. deltoideus	of m. subcoracoscapularis, m. deltoideus
scapularis, m. coracobrachialis brevis, m.	clavicularis, posterior portion of m.
coracobrachialis longus (rotation (leading	pectoralis, m. biceps brachii, m. triceps
edge upwards)	brachii (leading edge downwards)
m. biceps (retraction, depression)	m. triceps (elevation, protraction)
m. extensor digitorum communis (extension	m. flexor digitorum longus (flexes digit I-V)
metacarpals)	
humeral triceps head (offsets ulna slightly	m. flexor carpi ulnaris (displaces ulnar side
dorsally), m. extensor carpi ulnaris (offsets	of carpus ventrally, eventually flexes
ulna dorsally, or eventually extends	metacarpal V)
metacarpal V)	
m. supinator longus and extensor carpi	m. flexor carpi radialis (flexes metacarpal 1
radialis (offsets radius or eventually the	or offsets the radial carpal side ventrally),
radial carpal side dorsally)	m. pronator teres (offsets radius ventrally),





m. brachialis (offsets radius slightly
ventrally)

1



Table 3(on next page)



Agonistic and antagonistic femur muscles of Cryptoclidus eurymerus (IGPB R 324)



agonists	antagonists
m. puboischiofemoralis internus (pubis,	m. puboischiofemoralis externus (ischium),
vertebral column) (protraction, elevation)	m. adductor femoris, m. flexor tibialis
	internus (ischium), m. flexor tibialis
	externus (ischium), m. ischiotrochantericus,
	m. puboischiotibialis (retraction,
	depression)
m. puboischiofemoralis externus (pubis,	m. puboischiofemoralis internus (ischium,
anterior) (protraction, and depression)	ilium), m. caudifemoralis brevis and m.
	caudifemoralis longus, m. iliofibularis, m.
	iliotibialis, m. iliofemoralis, m. flexor
	tibialis externus (ilium), m. flexor tibialis
	internus (vertebral column) (retraction
	elevation)
m. ambiens (protraction), m. pubotibialis	m. iliofibularis (elevation, retraction)
(protraction)	
m. puboischiofemoralis externus (pubis), m.	m. puboischiofemoralis externus (ischium),
puboischiofemoralis internus (ischium,	m. puboischiofemoralis internus (pubis), m.
ilium), iliofemoralis, iliotibialis (rotates	adductor femoris, m. ischiotrochantericus,
flipper leading edge up), m. ambiens and m.	m. flexor tibialis internus, m. caudifemoralis
pubotibialis (rotates flipper leading edge up,	brevis, m. caudifemoralis longus, m. flexor
if tibia below origin area),)	tibialis externus, puboischiotibialis, m.
	iliofibularis (rotates flipper leading edge
	down), m. ambiens and m. pubotibialis
	(rotates flipper leading edge down, if tibia
	above origin area)
m. extensor digitorum longus (digital	m. gastrocnemius internus + m.
extensor), femorotibialis (offsets tibia	gastrocnemius externus, m. flexor digitorum
dorsally)	longus (digital flexors)



Table 4(on next page)

Muscle forces of *Cryptoclidus eurymerus* (IGPB R 324) humerus by superposition of FESA load cases



muscle	muscle force [N]
m. supracoracoideus	6000
m. coracobrachialis brevis	4800
m. coracobrachialis longus	3600
m. deltoideus clavicularis	1500
m. deltoideus scapularis	1649
m. scapulohumeralis anterior	2400
m. scapulohumeralis posterior	1920
m. brachialis	324
m. triceps humeral head	275
m. pectoralis	9600
m. subcoracoscapularis	4422
m. latissimus dorsi	3918
m. extensor carpi ulnaris	1000
m. extensor digitorum communis	6000
m. extensor carpi radialis	1000
m. pronator teres	640
m. flexor carpi ulnaris	3000
m. flexor digitorum longus	1500
m. flexor carpi radialis	1500



Table 5(on next page)

Muscle forces of *Cryptoclidus eurymerus* (IGPB R 324) femur by superposition of FESA load cases



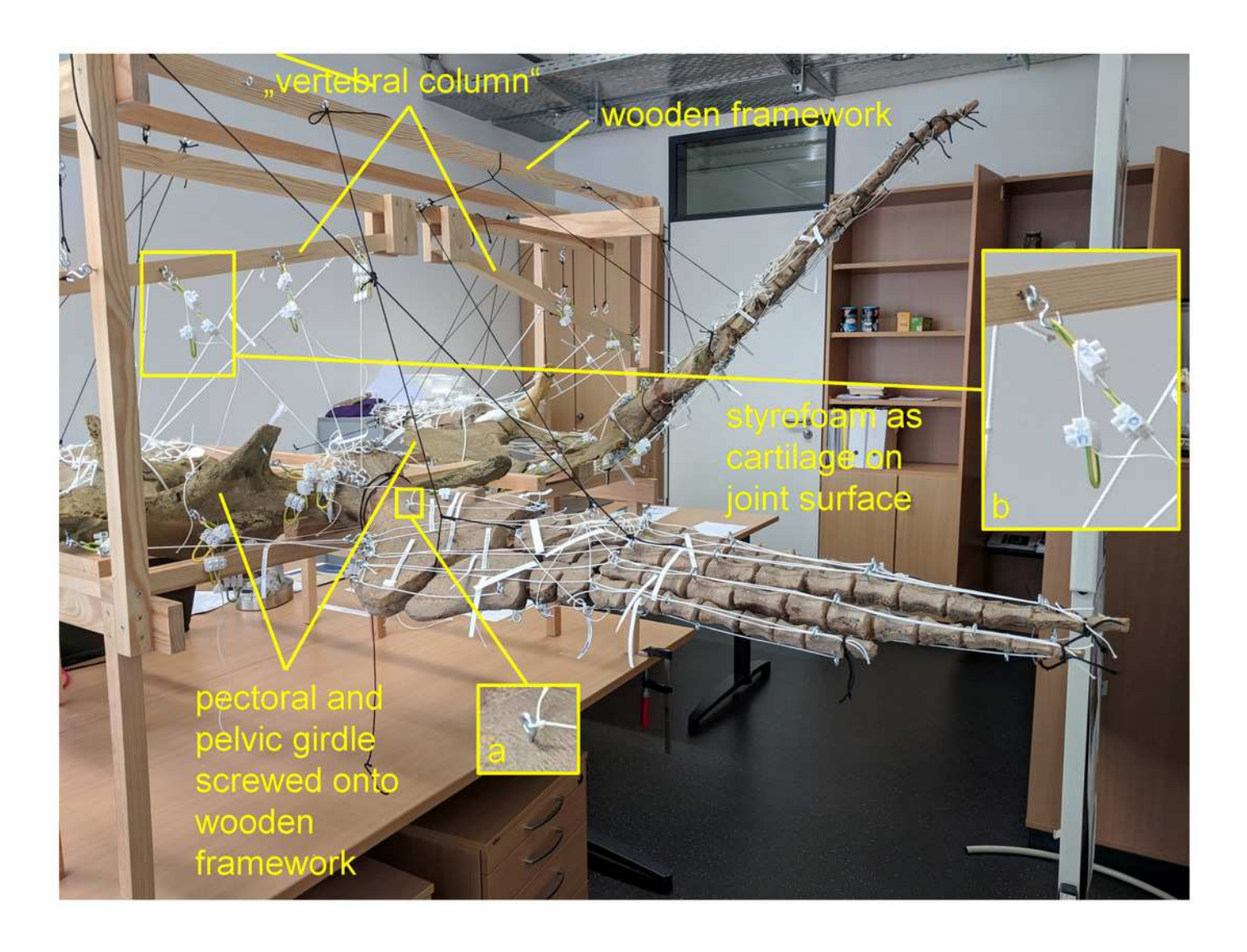
muscle	muscle force [N]
m. puboischiofemoralis externus	7878
m. puboischiofemoralis internus	7611
m. femorotibialis	1521
m. adductor femoris	3938
m. ischiotrochantericus	984
m. iliofemoralis	253
m. caudifemoralis brevis	506
m. caudifemoralis longus	507
m. extensor digitorum communis	1014
m. gastrocnemius	1176
m. flexor digitorum longus	786

1

F

Analog model demonstrating LOA of *Cryptoclidus eurymerus* (IGPB R 324) fore- and hindflipper.

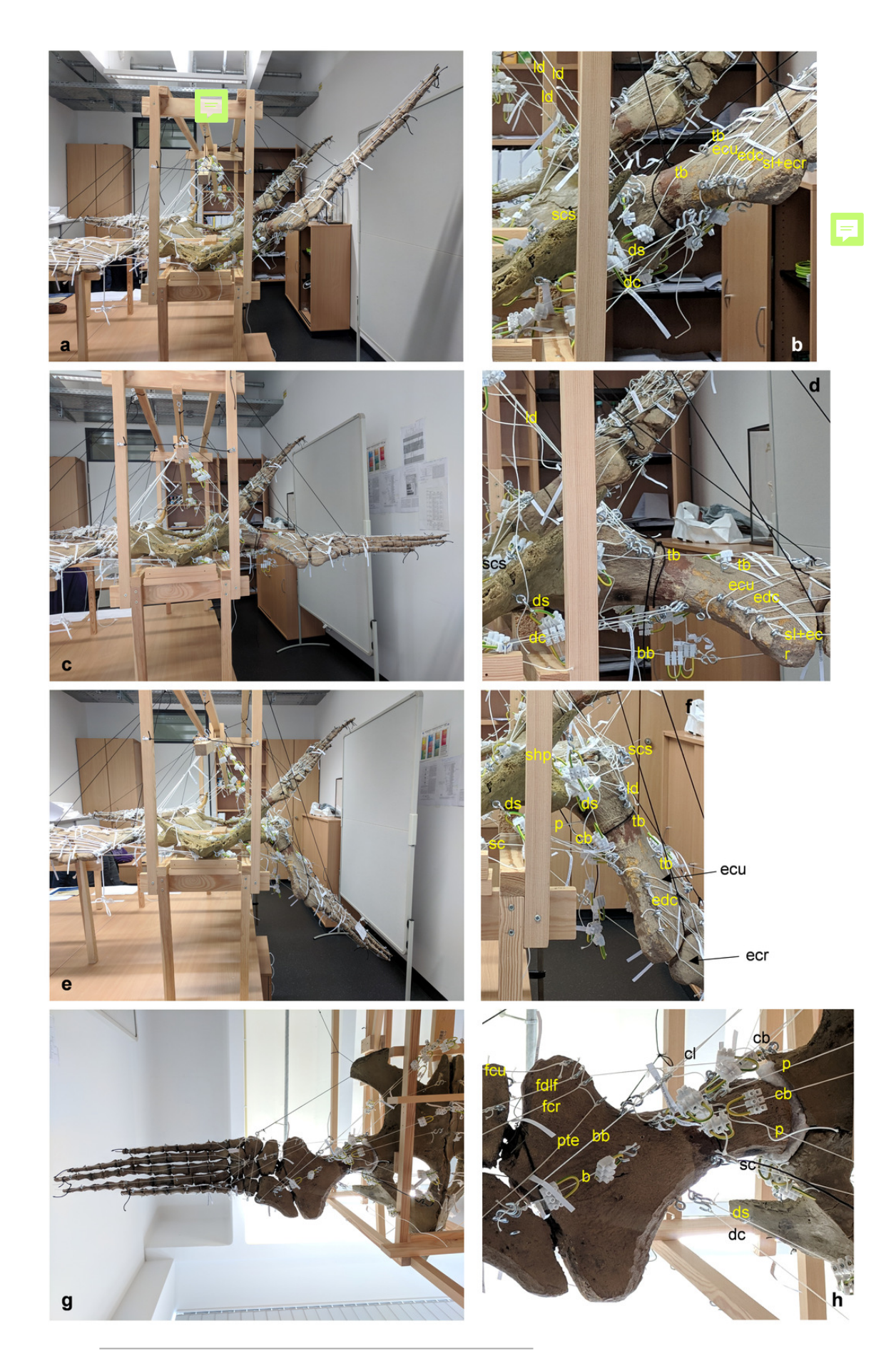
Pectoral and pelvic girdle were fixed on a wooden frame. Thick styrofoam was placed into the glenoid and acetabulum joint cavity. Black threads helped to fix the flippers in their respective position. White threads represent LOA: a) screw eye pins were screwed into muscle attachment surfaces. Three electrical terminal strips were attached to one end. With hooks attached to each end of the thread, LOA were hung into the screw eye pins.





LOA of Cryptoclidus eurymerus (IGPB R 324) foreflipper in anterior and ventral view.

Pictures on the left (a, c, e, g) show an overview over all flipper muscles. Pictures on the right focus on the humerus muscles. a) and b) during maximum dorsal excursion in anterior view. c) and d) in the neutral position in anterior view. e) and f) during maximum ventral excursion in anterior view. g) and h) ventral view of the neutral foreflipper position. Abbreviations: b, Musculus brachialis; bb, Musculus biceps brachii; cb, Musculus coracobrachialis brevis; cl, Musculus coracobrachialis longus; dc, Musculus deltoideus clavicularis; ds, Musculus deltoideus scapularis; ecu, Musculus extensor carpi ulnaris; edc, Musculus extensor digitorum communis; fcr, Musculus flexor carpi radialis; fcu, Musculus flexor carpi ulnaris; fdlf, Musculus flexor digitorum longus (foreflipper); ld, Musculus latissimus dorsi; p, Musculus pectoralis; pte, Musculus pronator teres; sc, Musculus supracoracoideus; scs, Musculus subcoracoscapularis; shp, Musculus scapulohumeralis posterior; sl and ecr, Musculus supinator longus and Musculus extensor carpi radialis; tb, Musculus triceps brachii.



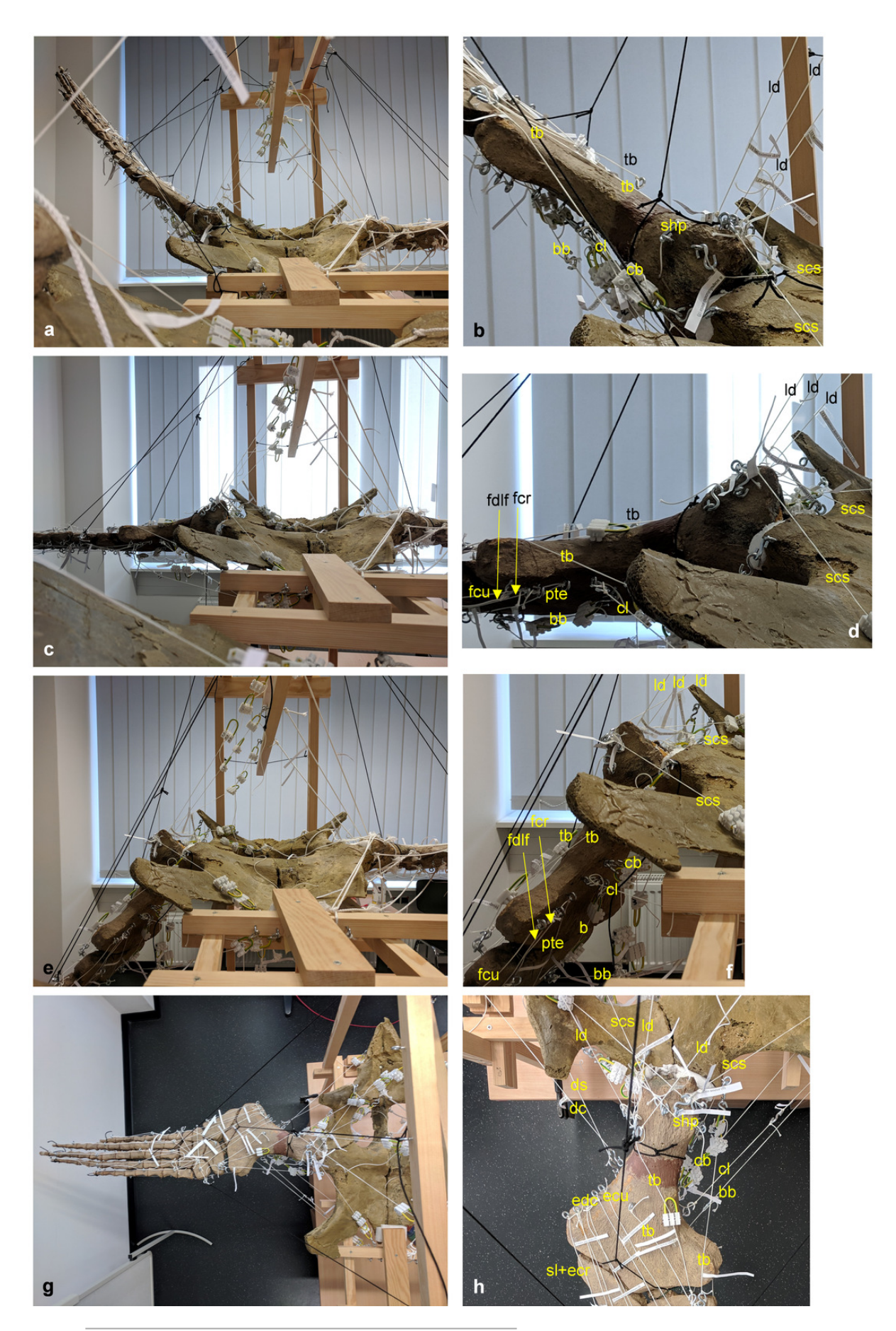
PeerJ reviewing PDF | (2021:02:58478:0:1:NEW 15 Mar 2021)



LOA of Cryptoclidus eurymerus (IGPB R 324) foreflipper in posterior and dorsal view.

Pictures on the left (a, c, e, g) show an overview over all flipper muscles. Pictures on the right focus on the humerus muscles. a) and b) during maximum dorsal excursion in posterior view. c) and d) in the neutral position in posterior view. e) and f) during maximum ventral excursion in posterior view. g) and h) dorsal view of the neutral foreflipper position.

Abbreviations: b, Musculus brachialis; bb, Musculus biceps brachii; cb, Musculus coracobrachialis brevis; cl, Musculus coracobrachialis longus; dc, Musculus deltoideus clavicularis; ds, Musculus deltoideus scapularis; ecu, Musculus extensor carpi ulnaris; edc, Musculus extensor digitorum communis; fcr, Musculus flexor carpi radialis; fcu, Musculus flexor carpi ulnaris; fdlf, Musculus flexor digitorum longus (foreflipper); ld, Musculus latissimus dorsi; pte, Musculus pronator teres; scs, Musculus subcoracoscapularis; shp, Musculus scapulohumeralis posterior; sl and ecr, Musculus supinator longus and Musculus extensor carpi radialis; tb, Musculus triceps brachii.



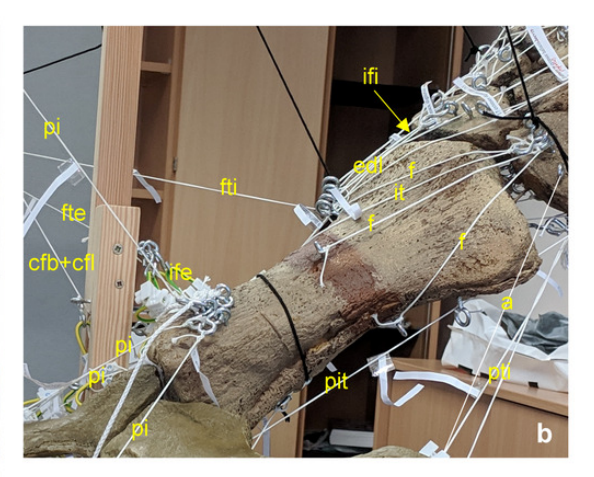
PeerJ reviewing PDF | (2021:02:58478:0:1:NEW 15 Mar 2021)



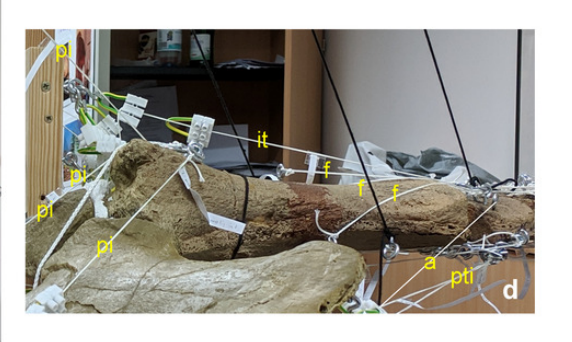
LOA of Cryptoclidus eurymerus (IGPB R 324) hindflipper in anterior and ventral view.

Pictures on the left (a, c, e, g) show an overview over all flipper muscles. Pictures on the right focus on the femur muscles. a) and b) during maximum dorsal excursion in anterior view. c) and d) in the neutral position in anterior view. e) and f) during maximum ventral excursion in anterior view. g) and h) ventral view of the neutral hindflipper position. Abbreviations: a, Musculus ambiens; af, Musculus adductor femoris; cfb, Musculus caudifemoralis brevis; cfl, Musculus caudifemoralis longus; edl, Musculus extensor digitorum longus; f, Musculus femorotibialis; fdlh, Musculus flexor digitorum longus (hindflipper); fte, Musculus flexor tibialis externus; fti, Musculus flexor tibialis internus; gi and ge, Musculus gastrocnemius internus and Musculus gastrocnemius externus; i, Musculus ischiotrochantericus; ife, Musculus iliofemoralis; ifi, Musculus iliofibularis; it, Musculus iliotibialis; pe, Musculus puboischiofemoralis internus; pit, Musculus puboischiotibialis; pti, Musculus pubotibialis.

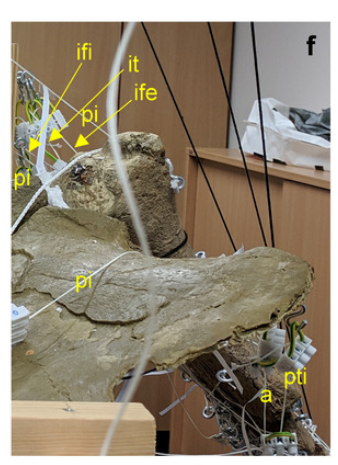




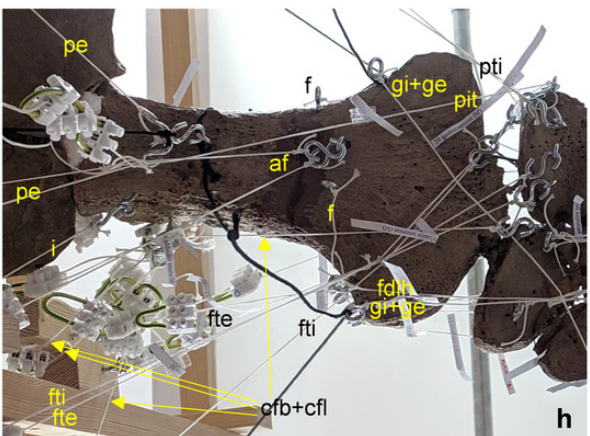










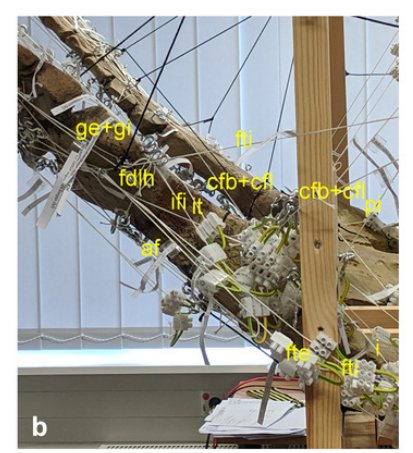


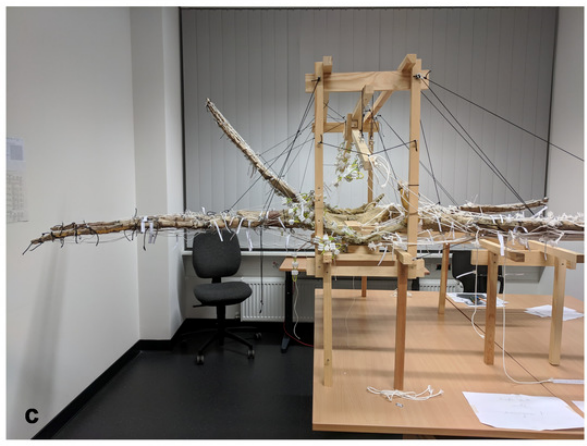


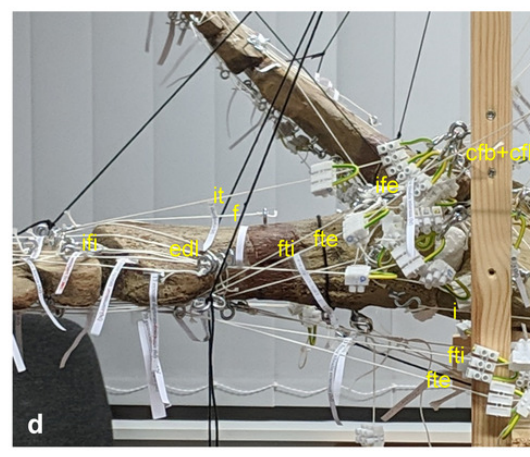
LOA of Cryptoclidus eurymerus (IGPB R 324) hindflipper in posterior and dorsal view.

Pictures on the left (a, c, e, g) show an overview over all flipper muscles. Pictures on the right focus on the femur muscles. a) and b) during maximum dorsal excursion in posterior view. c) and d) in the neutral position in posterior view. e) and f) during maximum ventral excursion in posterior view. g) and h) dorsal view of the neutral hindflipper position. Abbreviations: a, Musculus ambiens; af, Musculus adductor femoris; cfb, Musculus caudifemoralis brevis; cfl, Musculus caudifemoralis longus; edl, Musculus extensor digitorum longus; f, Musculus femorotibialis; fte, Musculus flexor tibialis externus; fti, Musculus flexor tibialis internus; i, Musculus ischiotrochantericus; ife, Musculus iliofemoralis; ifi, Musculus iliofibularis; it, Musculus iliotibialis; pe, Musculus puboischiofemoralis externus; pi, Musculus pubotibialis.

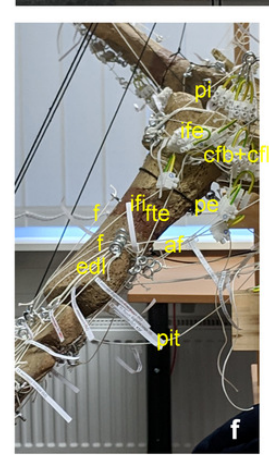




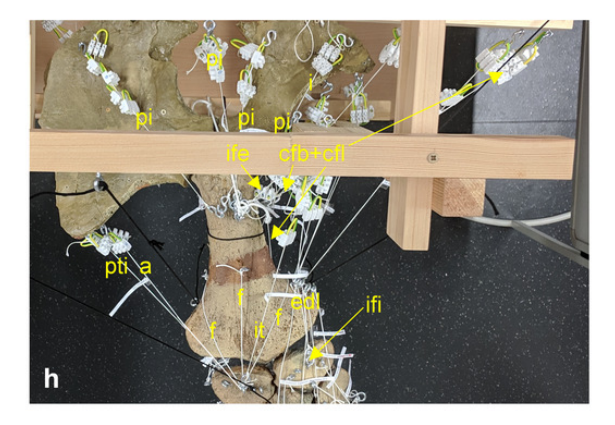








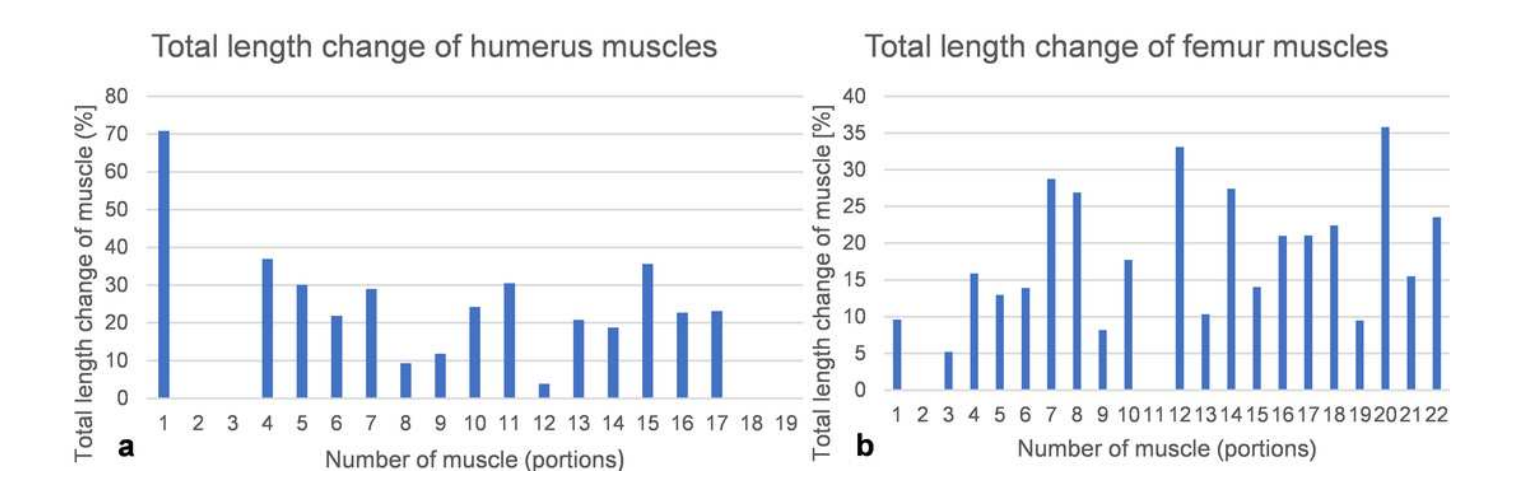






Total length change of muscles. a) humerus muscle(s) (portions) and b) femur muscle(s) (portions).

a) and b) Locomotory muscles that insert into or originate from humerus and femur cover the whole spectrum of maximum total muscle length change of vertebrate muscle well, ranging from no measurable total length change (of muscles with a complex architecture) to around 40% of total length change of muscle (typical for approximately parallel-fibred muscles; marked by turquoise line) (Biewener, Corning & Tobalske, 1998; Biewener & Roberts, 2000). Note in a) how m. deltoideus scapularis (1), if it originates from the scapula, would show an unphysiological total length change of muscle. If it originates from the ventral scapula (2), total muscle length change drops down into the physiological spectrum and ranges within the measuring error (typical for muscles with a complex internal architecture).



FESA of *Cryptoclidus eurymerus* (IGPB R 324) humerus and femur. a)-d) humerus, e)-h) femur.

a), e) contour drawings of humerus and femur and lines of action of the respective muscles in ventral view which were derived by spanning threads into the flipper skeleton of Cryptoclidus. b) f) meshed volumetric FE models with force vectors in ventral view which were transferred from the contour drawings (a, e). FESA superpositions of both load cases (down- and upstroke) in c), d) in dorsoventral view and g), h) in anteroposterior view. The colour spectrum codes the compressive stress in MPa. Please note how regions of lower compressive stress match with regions of spongy bone and regions of higher compressive stress match with cortical bone. Abbreviations: af, Musculus adductor femoris; b, Musculus brachialis; bb, Musculus biceps brachii; cb, Musculus coracobrachialis brevis; cfb, Musculus caudifemoralis brevis; cfl, Musculus caudifemoralis longus; cl, Musculus coracobrachialis longus; dc, Musculus deltoideus clavicularis; ds, Musculus deltoideus scapularis; f, Musculus femorotibialis; fcr, Musculus flexor carpi radialis; fcu, Musculus flexor carpi ulnaris; fdlf, Musculus flexor digitorum longus (foreflipper); fdlh, Musculus flexor digitorum longus (hindflipper); fte, Musculus flexor tibialis externus; fti, Musculus flexor tibialis internus; gi and ge, Musculus gastrocnemius internus and Musculus gastrocnemius externus; i, Musculus ischiotrochantericus; p, Musculus pectoralis; pe, Musculus puboischiofemoralis externus; pit, Musculus puboischiotibialis; pte, Musculus pronator teres; pti, Musculus pubotibialis; sc, Musculus supracoracoideus.



